T.C.

BAHCESEHIR UNIVERSITY

GRADUATE SCHOOL

DEPARTMENT OF ELECTRICAL & ELECTRONICS ENGINEERING

A COMPARATIVE ANALYSIS OF SILICON CARBIDE AND GALLIUM NITRIDE AS ALTERNATIVES TO SILICON IN HIGH-POWER SEMICONDUCTOR APPLICATIONS USING QSPICE

MASTER'S THESIS

MOHAMAD ALI BILAL

ISTANBUL 2025

T.C.

BAHCESEHIR UNIVERSITY

GRADUATE SCHOOL

DEPARTMENT OF ELECTRICAL & ELECTRONICS ENGINEERING

A COMPARATIVE ANALYSIS OF SILICON CARBIDE AND GALLIUM NITRIDE AS ALTERNATIVES TO SILICON IN HIGH-POWER SEMICONDUCTOR APPLICATIONS USING QSPICE

MASTER'S THESIS

MOHAMAD ALI BILAL

THESIS ADVISOR

Prof. Dr. ŞEREF KALEM

ISTANBUL 2025

T.C.

BAHCESEHIR UNIVERSITY

GRADUATE SCHOOL

MASTER THESIS APPROVAL FORM

Program Name:	ELECTRICAL AND ELECTRONICS ENGINEERING (ENGLISH, THESIS)
Student's Name and Surname:	MOHAMAD ALI BILAL
Name Of The Thesis:	A Comparative Analysis of Silicon Carbide and Gallium Nitride as Alternatives to Silicon in High Power Applications Using QSPICE
Thesis Defense Date:	08/01/2025

This thesis has been approved by the Graduate School which has fulfilled the necessary conditions as Master thesis.

Assoc. Prof. Dr. Yücel Batu SALMAN

Institute Director

This thesis was read by us, quality and content as a Master's thesis has been seen and accepted as sufficient.

	Title/Name	**Institution**	**Signature**
Thesis Advisor's	Prof.Dr. Şeref KALEM	Bahçeşehir University	
Member's	Prof. Dr. Bülent ULUĞ	Bahçeşehir University	
Member's	Dr. Öğr. Üyesi Lida KOUHALVANDI	Doğuş University	

I hereby declare that all information in this document has been obtained and presented in accordance with academic rules and ethical conduct. I also declare that, as required by these rules and conduct, I have fully cited and referenced all material and results that are not original to this work.

Name, Last Name: MOHAMAD ALI BILAL

Signature:

ABSTRACT

A COMPARATIVE ANALYSIS OF SILICON CARBIDE AND GALLIUM NITRIDE AS ALTERNATIVES TO SILICON IN HIGH-POWER SEMICONDUCTOR APPLICATIONS USING QSPICE

MOHAMAD ALI BILAL

Electrical And Electronics Engineering Master's Program

Supervisor: Prof. Dr. ŞEREF KALEM

January 2025, 53 Pages

This master thesis investigates the performance of Silicon (Si), gallium nitride (GaN), and silicon carbide (SiC) MOSFETS in a flyback converter application. A comparative analysis was conducted to evaluate the performance of each semiconductor material under various operating conditions. key parameters such as efficiency, MOSFET power dissipation, thermal performance, and output voltage regulation was simulated and studied using QSPICE. The results show that GaN MOSFETS proved its enhanced working capability in high-frequency applications. Moreover, SiC showed its suitability for high-power applications and provided a tradeoff between price and capability. On the other hand, despite its low cost, Si remains primarily suited for low-power and frequency applications.

Key Words: Silicon, Silicon Carbide, Gallium Nitride, High-power applications, Flyback converter.

ÖZET

QSPICE KULLANILARAK YÜKSEK GÜÇLÜ YARIİLETKEN UYGULAMALARINDA SİLİSYUMA ALTERNATİF OLARAK SİLİSYUM KARBÜR VE GALYUM NİTRİDİN KARŞILAŞTIRMALI ANALİZİ

MOHAMAD ALI BILAL
Electric-Electronic Engineering Yüksek Lisans Programı

Tez Danışmanı: PROF. Dr. ŞEREF KALEM

Ocak 2025, 53 sayfa

Bu yüksek lisans tezi, bir flyback dönüştürücü uygulamasında Silikon (Si), Gallium Nitrid (GaN) ve Silikon Karbür (SiC) MOSFET'lerinin performansını araştırmaktadır. Her bir yarı iletken malzemenin çeşitli çalışma koşullarındaki performansını değerlendirmek için karşılaştırmalı bir analiz yapılmıştır. Verimlilik, MOSFET güç kaybı, ısıl performans ve çıkış voltajı düzenlemesi gibi ana parametreler QSPICE kullanılarak simüle edilmiş ve incelenmiştir. Sonuçlar, GaN MOSFET'lerinin yüksek frekanslı uygulamalarda geliştirilmiş çalışma yeteneğini kanıtladığını göstermektedir. Ayrıca, SiC'nin yüksek güçlü uygulamalar için uygunluğunu ve fiyat ile kapasite arasında bir denge sağladığını göstermektedir. Diğer taraftan, düşük maliyetine rağmen, Si daha çok düşük güç ve frekanslı uygulamalar için uygun kalmaktadır.

Anahtar Kelimeler: Silikon, Silikon Karbür, Gallium Nitrid, Yüksek Güç Uygulamaları, Flyback Dönüştürücü.

Dedicated to my Family, Friends, and Mentors whose unwavering support and guidance made this journey possible.

ACKNOWLEDGEMENTS

I wish to express my deepest gratitude to my supervisor, Prof. Dr. Şeref Kalem, for his guidance, advice, criticism, encouragement, and insight throughout the research.

I would like to give special thanks to my parents, SAMEER BILAL and SUHAIR BANDAR, whose unconditional love, support, and belief in me have been my greatest source of strength throughout this journey.

TABLE OF CONTENTS

LIST OF TABLES

TABLES

LIST OF FIGURES

FIGURES

Chapter 1
Introduction

1.1 Theoretical Framework

Semiconductors are used virtually everywhere in today's technology, from mobile phones and laptops to cars, satellites, aircraft, and pacemakers. They are the invisible building blocks that drive and shape much of modern life. Semiconductors, which sit between insulators and conductors, are crucial in allowing or blocking electrical current. In electronic devices, semiconductors facilitate advancements in diverse sectors including communications, computing, healthcare, transportation, military defense, and clean energy (Glashauser & Kreutzer, 2023). Over the decades, silicon (Si) has been the most popular Semiconductor material used in Power electronic switches (PES) due to its superior characteristics. It all started in late December 1947 when Shockley, Bardeen, and Brattain used Germanium (Ge) to create the point-contact transistor (Hoddeson,1981). A couple of years later, with the benefit of the invention and improvement of technology, Silicon (Si) came into the picture and dominated the power industry. However, Silicon (Si) has rapidly reached its theoretical performance limits concerning efficiency, switching speed, and size. The growing demand for more efficient systems in the power electronics sector has led to the need for more reliable and compact designs. Recently, Wide band gap (WBG) semiconductors such as Silicon Carbide (SiC), and Gallium Nitride (GaN), have seen growing use in improving the performance of power electronics, particularly in High power, high-frequency, and high-temperature applications (Sheng & Guo, 2012). These materials allow power converters to function at higher voltages, temperatures, and switching frequencies compared to conventional Silicon (SI) devices. The enhanced characteristics of WBG semiconductor materials contribute significantly to advancement in power electronics, energy efficiency, miniaturization of electronic devices, cost reduction, and longer device lifespans (Pullabhatla, Bobba, & Yadlapalli, 2020).

SiC and GaN feature superior material properties compared to silicon, as demonstrated in Table 1 below.

Table 1

Semiconductor Materials Properties (Pullabhatla et al., 2020) (Udabe, Etxaburu, & Garrido, 2023)

Electrical property	Silicon (Si)	Silicon carbide (SiC)	Gallium Nitride (GaN)	Units
Band Gap	1.1	3.26	3.44	eV
Thermal Conduction	1.5	3.7	1.3	W/cm. K
Electron mobility	1300	900	900-1200	$Cm^2/V.s$
Electron Saturation Velocity	10	22	25	$(10^6)\ cm/sec$
Critical field	0.3	3	3.5	$(10^6)\ V/cm$

Table 1 above compares the different properties of Si, SiC, and GaN semiconductor materials. The definitions of each are listed in section 1.6 below.

1.2 Statement of the Problem

Modern technology expansion has raised the demand for more reliable and efficient systems. Historically, Silicon (Si) has long been the primary semiconductor material used in power electronics. However, the increasing requirements for higher operating voltages and frequencies in contemporary applications have highlighted the advantages of wide bandgap (WBG) semiconductor materials such as SiC and GaN. These materials are widely acknowledged for their superior performance in high-power environments where silicon reaches its limitations. Furthermore, with all the new and different flavors of transistors, it's becoming harder for engineers to decide on the best option for their designs. Engineers need to select the correct MOSFET to meet their design requirements. Some products or industries prioritize efficiency, while others prioritize cost or physical dimensions. Some transistors perform better than others but may fail at higher temperatures. Others excel, but only in high-frequency applications.

1.3 Purpose of the Study

This thesis aims to perform a comparative analysis of Silicon Carbide (SiC) and Gallium Nitride (GaN) as alternatives to Silicon (Si) in high-power semiconductor applications, with a particular focus on their performances in a Flyback converter

design. Using QSPICE, a circuit simulation software, the efficiency of the semiconductor materials will be evaluated to examine the advantages of wide band gap material under various operating conditions. The simulation will study the efficiency, MOSFET power dissipation, breakdown voltage, thermal performance, and output voltage regulation of different Si, SiC, and GaN devices under various operating conditions. Also, a real-world market cost analysis of the chosen devices is conducted to account for the cost-saving considerations when evaluating.

1.4 Hypothesis/Research Questions

- Are the GaN MOSFETs more efficient than Si MOSFETS?
- Are the GaN MOSFETs more suitable than Si MOSFETS for high-frequency applications?
- Are the SiC MOSFETs more reliable than Si MOSFETs for high-voltage and high-temperature applications?

1.5 Significance of the Study

The significance of this study is that it compares different transistors based on various semiconductor materials, not just using datasheet values but through circuit simulations of a practical, real-life application. The circuit components connected to the transistor (MOSFET) affect its behavior in ways that cannot be easily evaluated from the datasheet. Additionally, different manufacturers' datasheets provide the device parameters under different test conditions, making it difficult to compare different devices.

Furthermore, this study could serve as a foundation for future research aimed at automating the analysis presented here, enabling it to be extended to a larger database of transistors. As the design and simulation aspects of the study are presented in detail, this study could also be useful for students and other researchers.

1.6 Definitions

- Band gap: The energy difference between the highest occupied energy state of the valence band and the lowest occupied energy state of a conduction band in a semiconductor material *(Pullabhatla et al., 2020)*.
- Thermal conductivity: a material's ability to transfer heat through itself.
- Electron mobility: the measure of how easily electrons can move through a material when an electric field is applied.

- Electron saturation velocity: the maximum velocity at which electrons can move through a material when an electric field is applied.
- Critical field: The electric field strength at which a material begins to breakdown or avalanche causing uncontrolled conditions (Ahmed, Khan, Butt, Kazanskiy, & Khonina, 2022).
- Si: Silicon
- SiC: Silicon Carbide
- GaN: Gallium Nitride
- Crossover frequency: The frequency at which a power supply's open loop frequency response crosses the 0dB point. It defines how fast the power supply reacts to changes in the load demand (RAJU, 2020).
- Phase Margin: One of two key stability measurements of the power supply. It's the phase measurement at the frequency at which the loop gain crosses 0dB (RAJU, 2020).
- Gain Margin: One of two key stability measurements of the power supply. It's the gain measurement at the frequency at which the open loop phase crosses 180 degrees (RAJU, 2020).
- Flyback converter: A common power supply or DC-DC converter topology. It falls under the Buck-Boost topologies.
- IGBT: Isolated Gate Bipolar Transistor
- JFET: Junction Field Effect Transistor
- FET: Field Effect Transistor

The thesis is structured as follows. Chapter 1, introduction, provides an overview of Si, SiC, and GaN as types of semiconductor materials and their key properties, followed by a detailed comparison between them. Additionally, the objective and importance of this research are explained, highlighting the relevance of these materials in modern applications. Chapter 2, the literature review, studies the existing research on Si, SiC, and GaN semiconductor materials, with a focus on their role in power electronics. Key advancements in wide bandgap semiconductors and their performance in high-power applications are analyzed. The review highlights the strengths and limitations of these materials and identifies gaps in the current literature

that this thesis aims to address, particularly in optimizing power conversion systems. Chapter 3, Methodology, outlines the methods and techniques used to conduct the research. It details the design and simulation of circuits using QSPICE, including comparing silicon, silicon carbide (SiC), and gallium nitride (GaN) semiconductors. The parameters and conditions for the simulations are described, along with the data collection and analysis procedures. Chapter 4, Results and Discussion, presents the simulations' findings and discusses the research objectives' results. A detailed comparison of the performance of silicon, SiC, and GaN in terms of efficiency, power density, and thermal properties is provided. Finally, chapter 5, conclusion and future works, this chapter summarizes the key findings of the research and their significance in advancing power electronics. It also discusses the limitations of the study and suggests potential areas for future research.

Chapter 2

Literature Review

The need for efficient, reliable, high-quality, and compact power systems in modern electronics has driven the development of various power conversion technologies. DC-DC converters, in particular, play a crucial role in regulating and transforming electrical energy. Approximately 80% of electrical energy consumption is estimated to flow through a power converter (Czarkowski, 2011, pp. 249–263). These systems heavily depend on power semiconductor switches to achieve high efficiency, reliability, and performance. These switches not only enhance the overall efficiency by minimizing the total power losses but also contribute to the effective thermal management of the system (Picard, 2010). Depending on the type of semiconductor material used, the device lifespan is increased, and their role is to ensure the ability to handle higher breakdown voltage and current. In addition to these benefits, power semiconductor switches contribute to faster switching speeds and support more compact designs. In the last decades, plenty of studies and investigations were implemented to study the benefit of having a wider bandgap on the system. According to SBURLAN, VASILE, and TUDOR (2021), the authors studied and analyzed how various semiconductor devices used to manufacture electric systems of an electric vehicle can affect energy efficiency. Si, SiC, e-GaN, and d-GaN power semiconductor devices were used, and each has its properties. For comparison purposes, the authors employed the figure of merit (FOM), a specific calculation metric used to evaluate and compare a system's performance, efficiency, and effectiveness. In their study, they used FOM to estimate the device power losses by the product of the semiconductor materials drain-source resistance (Rds-on) and the total charge (Q_{GD}). Calculations were made for all the devices for both conduction and switching losses. The authors ensured that the devices chosen were close to each other regarding the breakdown voltage, where the Si, e-GaN, and d-GaN had a 650V drain to source breakdown voltage (V_{DS}), and 1200V for SiC. Furthermore, the calculations were done with a fixed voltage supply, current induced, and switching frequency for all the devices for the proper evaluation. The recorded values of FOM showed a significant difference between the different types of power semiconductor devices used. It was recorded that devices based on SiC and GaN had much fewer power losses

than Si-type power devices. Moreover, Sburlan and his colleagues compared the materials' parasitic elements that caused the losses in the system. Due to SiC and GaN having less total charge and drain-source resistance, they overcome the silicon. Another key characteristic is the input capacity (C_{iss}), which is a combination of gate-to-drain capacitance (C_{GD}) and gate-to-source capacitance (C_{GS}). The Ciss should be charged or discharged to change the gate voltage to alternate the switch between the ON and OFF states. The wide bandgap semiconductor devices in this study showed decreased values of Ciss compared to silicon, which means less power is required to actuate the gate. Also, the reverse transfer capacity (C_{rss}) of SiC and GaN are less than Si, guaranteeing the danger of a sudden gate opening. Lastly, the output capacitance (C_{oss}) directly affects the device's switching losses, which are recorded less for the wide band gap materials than for silicon. As a result, SiC and GaN semiconductor devices recorded fewer total losses than Si. For the same voltage and current conditions, the Enhancement GaN (e-GaN) power device showed a significant decrease in the conduction losses by around 60% compared to the Si-type device.

According to Rai (2020), power engineers face two critical limitations when choosing the best devices for their design. The first limitation is that power performance highly depends on its interaction with the circuit. This means that selecting the optimum value of a device's parameters, such as Breakdown voltage, on-resistance, gate charge, gate capacitance, and FOM is insufficient for the overall performance of a device. Secondly, engineers might not be familiar with all the available power devices in the market, forcing them to overlook some excellent alternatives as they have a narrow range of devices because of their selection criteria. Therefore, a list of over 20,000 different field effect transistor (FET) devices from 33 manufacturers was considered in this study for power loss modelling. Switching losses, conduction losses, and diode reverse recovery losses were estimated based on the devices' datasheets. A special dashboard was used to plot the devices' total losses under various conditions. In this research, a 3 KW power converter was selected to demonstrate its performance under two different operating conditions. The first was having a drain-to-source voltage V_{DS} of 400 V, drain current I_D of 15A, a duty cycle of 50%, total gate resistance of 10 Ω, ambient temperature of 25°, gate-to-source voltage of 10V, and a varying switching frequency from 1KHz to 200KHz. The same

operating conditions were maintained in the second operating conditions, with the only changes being that the drain-to-source voltage increased to 800v and the drain current I_D reduced to 7.5A. The author has set a requirement for each operating condition, whereas the devices chosen for the first operation condition should have a breakdown voltage that rates between 600V-900V and a maximum power loss of 40W. For the second, the breakdown voltage rate is between 1100V and 1700V while maintaining a 40 W maximum power loss per device. The devices chosen for this study were Si MOSFETs, SiC FETs, and GaN HEMTs for both operation conditions.

Table 2

Research Data Collection 1: Operating at Vds=400V, Id=15A (Rai, 2020)

Freq.	Device Material	Device Rds-on (mΩ)	Lowest power loss (W)	Conduction losses (%)	Switching losses (%)	Diode reverse recovery (%)	Price ($)
1KHz	Si	18	4.06	50%	35%	15%	18.73
	SiC	9	2.21	46%	39%	15%	63.9
	GaN	41	4.8	96%	2.50%	1.50%	18.9
10KHz	Si	45	12.08	42%	36%	22%	8.6
	SiC	35	7.3	54%	36%	10%	16.2
	GaN	41	6.4	72%	17%	11%	21
20KHz	Si	45	18	27%	45%	28%	8.6
	SiC	35	10.65	37%	49%	14%	16.2
	GaN	41	8.2	56%	26%	18%	21

The study aims to compare Si, SiC, and GaN by modelling their power losses in different operating conditions. Table 2 above presents a detailed comparison of the selected semiconductor devices obtained by Rai. To start with, when operating at a low switching frequency of 1KHz, the conduction loss is the primary contributor to the total power loss as it highly depends on the Rds-on of a material. The lowest power loss between all devices available in today's market comes from SiC FET, with a power loss of 2.21 W at an Fs of 1kHz. The reason behind that is it's low on resistance, which made SiC a better choice compared to Si and GaN. However, when comparing the market price, SiC FET is 3.4 times more than both Si and GaN, which makes it a disadvantage if cost matters more in a design than efficiency. As seen from Table 2

above, the switching losses start to increase with the increase in switching frequency. Even though SiC has the lowest on-resistance when operating at both 10KHz and 20KHz switching frequencies, GaN has the lowest power loss among all market devices. This is because of the great combination of low on-resistance, low gate charge, and low diode reverse recovery that GaN semiconductor material possesses. But GaN's high market price makes SiC a good alternative as they both have a less than a watt difference in power loss.

Table 3

Research Data Collection 2: Operating at Vds= 400V, Id=15A (Rai, 2020)

Freq.	Device material	Device Rds-on (mΩ)	Lowest power loss (W)	Conduction losses (%)	Switching losses (%)	Diode reverse recovery (%)	Price ($)
100KHz	SiC	94	25	42%	43%	15%	11.6
	GaN (E-mode)	90	12.55	81%	19%	0%	16.54
		65	12.8	57%	43%	0%	-
	GaN (cascode)	41	22.4	-	-	-	21
		85	18	-	-	-	11.8
200KHz	SiC	142	38.7	41%	43%	16%	11.4
	GaN	90	15	68%	32%	0%	-

Table 3 above illustrates the effect of operating under high switching frequency on the device power loss modeling. It was observed by the author that no Si-based device met the power loss criterion of less than 40 W. For 100KHz and 200KHz operating frequencies, Enhancement mode (E-mode) GaN recorded significantly lower power loss values compared to both cascode mode GaN and SiC power devices. E-mode GaN HEMTs do not have a body diode, which means that they do not experience a reverse recovery charge during switching. As a result, reverse recovery losses are eliminated. As per any design requirement, the cascode mode GaN device with an 18W power loss for a market price of 11.8$ could provide significantly greater value for 100KHz operation. The researcher has observed that the E-mode GaN devices have shown better operation at higher frequencies followed by the cascode mode GaN. For lower frequencies, SiC could be a viable option in certain applications

where its power losses are comparable to GaN, but it offers a more competitive market price.

Table 4

Research Data Collection 3: Operating at Vds=800V, Id= 7.5A (Rai, 2020)

Freq.	Device Material	Device Rds-on (mΩ)	Lowest Power Loss (W)	Conduction Losses (%)	Switching Losses (%)	Diode Reverse Recovery (%)	Price ($)
1KHz	Si	330	14.29	65%	25%	10%	88
	SiC	50	1.64	48%	40%	12%	23.6
	SiC (Cascode)	11	2.5	12.50%	43.50%	44%	68.6
10KHz	SiC	90	5.2	49%	35%	16%	11.4
	SiC (Cascode)	90	5.4	47%	35%	18%	14.39
20KHz	SiC	110	7.4	42%	45%	13%	10.7
	SiC (Cascode)	90	8.3	30%	46%	24%	14.39

Table 5

Research Data Collection 4: Operating at Vds=800V, Id=7.5A (Rai, 2020)

Freq.	Device Material	Device Rds-on (mΩ)	Lowest Power Loss (W)	Conduction Losses (%)	Switching Losses (%)	Diode Reverse Recovery (%)	Price ($)
100KHz	SiC	294	18.8	44%	23%	33%	10.3
	SiC (Cascode)	180	21.8	23%	55%	22%	8.3
200KHz	SiC	468	28.7	46%	18%	36%	8.3
	SiC (Cascode)	180	38.5	13%	61%	26%	8.3

Rai (2020) did further analysis to observe the effect of changing the operating voltage when selecting the type of power device. As seen in Tables 4 and 5 above, GaN could not meet the criteria of having a high breakdown voltage between 1100 V to 1700 V. Therefore, SiC was the preferred choice when operating at higher voltages, as Si-based devices exhibit significantly higher power losses compared to SiC-based devices. The author observed this when E-mode SiC devices had the lowest power loss and the lowest cost at most of the operating frequencies. Moreover, devices with the

lowest Rds-on have not had the lowest power losses as power losses were arising from switching. Finally, e-mode SiC power devices had a superior performance in terms of higher voltages compared to other power semiconductor devices.

Several studies have been implemented on different applications throughout the years to observe the difference between WBG devices and normal Si devices. According to Shah et al. (2018), the authors have chosen a DC-DC buck-boost converter to implement a comparative analysis of the performance of Si IGBT, SiC JFET, and GaN FET. The aim was to study the effect of varying both the junction temperature and the switching frequency on each power semiconductor device's power loss and efficiency. The chosen devices for the study were GaN FET (TPH3207WS) with a 650V breakdown voltage and a 35mΩ Rds-on, SiC JFET (CM30065090D) with a 1200V breakdown voltage and a 65mΩ Rds-on, and Si IGBT (IGP20N65F5) with a 1200V breakdown voltage. Firstly, they evaluated the total power loss of each semiconductor material at different switching frequencies for three different junction temperatures of 25 °C, 100 °C, and 150 °C as demonstrated in Figure 1 below.

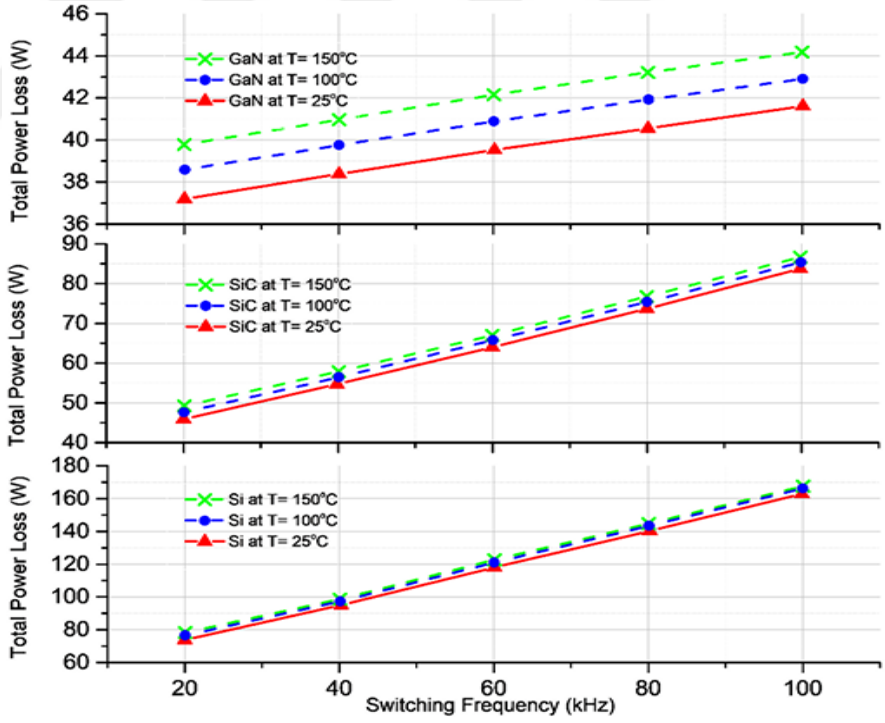

Figure 1. Total power loss Vs. switching frequency for 25 °C, 100 °C, 150 °C junction temperatures (Shah et al., 2018)

It can be seen that for all the devices in the three different junction temperatures, the total power loss increases with the increase of the Switching frequency.

Furthermore, the GaN FET-based converter recorded the lowest power losses among SiC JFET and Si IGBT power converters. For example, at 100KHz switching frequency and 150 °C junction temperature, GaN FET recorded a total power loss of around 44W while SiC JFET and Si IGBT recorded a total power loss of around 85W and 170 W respectively. Therefore, GaN FET has managed to reduce the total power loss by 49.4% compared to SiC JFET and around 74% compared to Si IGBT. Secondly, the authors have evaluated the efficiency of the system based on the losses obtained. Figure 2 below shows the efficiency of each semiconductor power converter for different switching frequencies. It can be seen that with the increase in the switching frequencies, the efficiency of a system decreases. The reason behind that is the increase in switching losses, which is an increase in total power loss. For switching frequency from 20KHz to 100KHz, the GaN FET-based converter achieved an outstanding efficiency between 96 % - 96.6%, the SiC JFET-based device attained a degree of efficiency between 92.5% - 95.3%, and the Si IGBT- based converter showed an efficiency range between 84% - 92.3%. This difference in efficiency levels concludes that GaN FET-based power converters overcome both SiC JFET and Si IGBT-based converters by 3.2% and 13.7% respectively of improved efficiency.

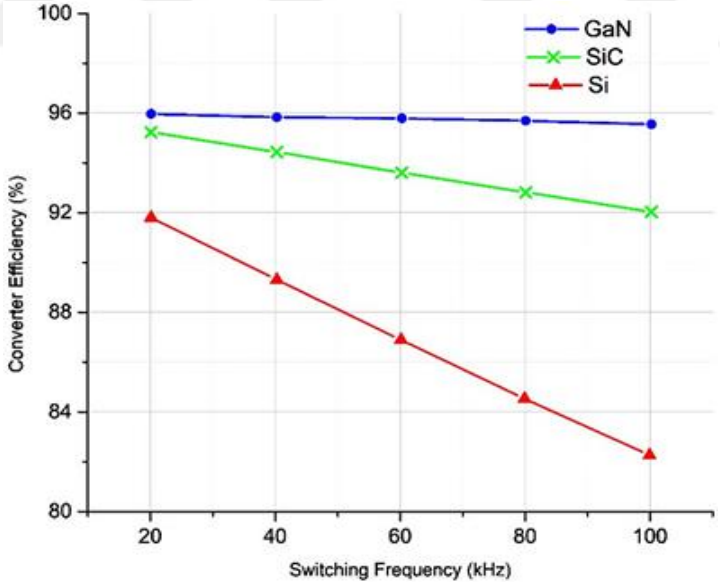

Figure 2. Si IGBT, SiC JFET, and GaN FET-based power converters efficiencies (Shah et al., 2018)

Moreover, the research team has studied the effect of changing the output power on the converter's efficiency while maintaining a fixed switching frequency and

junction temperature. Figure 3 below shows that GaN FET and SiC JFET converters recorded significantly better efficiency ranges than Si IGBT-based converters.

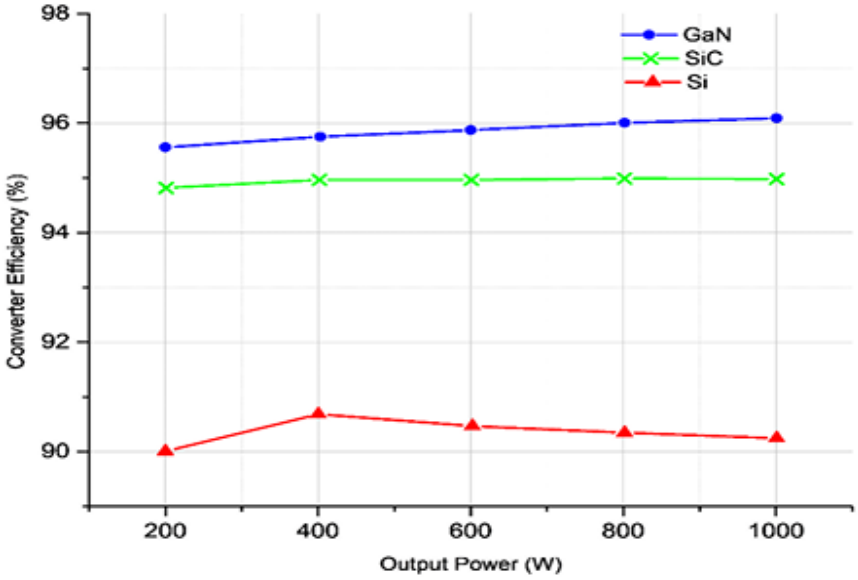

Figure 3. Converters efficiency for different output power and fixed switching frequency and junction temperature (Shah et al., 2018)

Additionally, the efficiency of the GaN FET converter is the only power device that kept increasing linearly with the increase of output power. For SiC JFET, the efficiency increased slightly up to 400 W, and after it maintained a fixed efficiency value. Regarding the Si IGBT converter, it started to decrease after hitting the 400W output power. Therefore, when looking at 1KW output power, the GaN power converter succeeded in improving the converter efficiency by 1.4% compared to SiC JFET and by 6.2% compared to Si IGBT. Finally, the authors fixed the switching frequency and variated the junction temperature from 25 °C to 150 °C to observe the effect of this change on the converter efficiency. Figure 4 below clearly shows that the increase in the junction temperature leads to a decrease in efficiency for all devices. The GaN FET-based power converter showed better efficiencies than SiC JFET and Si IGBT devices by 3.07% and 12.7%, respectively.

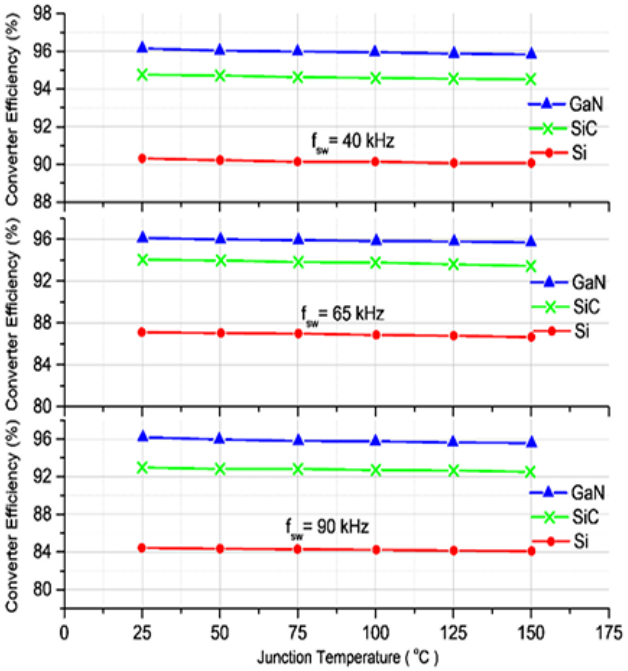

Figure 4. Converter efficiency with variated junction temperatures at different switching frequencies of 40KHz, 65KHz, and 90KHz (Shah et al., 2018)

Chapter 3
Methodology

3.1 Research Design

Using QSPICE, a software simulation tool, a Flyback power converter design will be implemented to test and compare the efficiency, MOSFET power dissipation, breakdown voltage, thermal performance, and output voltage regulation of different Si, SiC, and GaN devices under various operating conditions. Also, a real-world market cost analysis of the chosen devices is conducted to account for the cost-saving considerations when evaluating. Moreover, the output voltage of this design is regulated to maintain 12 V, regardless of variations in parameters such as input voltage and switching frequency.

Firstly, the efficiency of a system is a mathematical representation of the ratio of average instantaneous output power to average instantaneous input power. Using QSPICE, the average instantaneous powers are simulated, and the system's efficiency is calculated using a simple mathematical equation. Secondly, the power dissipation of each circuit component is simulated to identify and observe the high-dissipation components. By this, the average of the dissipated power is compared with the allowed power dissipation range provided in the datasheet for the element chosen, a MOSFET for example. Several factors might affect and reduce the efficiency of a circuit design, such as output capacitance, leakage inductance, load variations, etc. Therefore, the study will also focus on the MOSFET power dissipation effect on the overall efficiency of the design. By this, the performance of each semiconductor device can be effectively evaluated under the different operating conditions. Furthermore, the average MOSFET dissipated power will be used to calculate the effect of this heat dissipation on the rise in the component temperature. This is done by multiplying the thermal resistance (junction-to-case) provided in the datasheet by the MOSFET average power dissipated. This power dissipation will increase the MOSFET’s junction temperature beyond its initial operating temperature. After that, the new junction temperature is compared with the maximum allowable junction temperature specified in the MOSFET datasheet to ensure it remains within the acceptable range. Lastly, verifying a system's stability and the design's functionality highly depends on ensuring the proper operation within the breakdown voltage limits of a MOSFET. Each

MOSFET has unique design parameters, and the breakdown voltage represents its ability to handle high voltages before collapsing. The drain to source voltage (Vds) is simulated to compare and ensure that the Vds range is below the datasheet maximum allowed breakdown voltage. In this research, different types of MOSFET devices with varying materials of semiconductor, Si, SiC, and GaN, are chosen for comparison purposes, taking into consideration the properties of each. Additionally, a study of actual market prices will be implemented to evaluate the cost-effectiveness properties of the different semiconductor MOSFET devices used. The simulation will be done under various operating conditions, including fixed input voltage and varying switching frequencies. Also, a simulation study of a fixed switching frequency and variated input voltage are implemented to evaluate the performance of Si, SiC, and GaN semiconductor materials.

In real-life applications, loads rarely remain constant as they vary depending on consumer demands. This load variation introduces various barriers when designing a power converter, especially a Flyback converter. The proposed design must consistently deliver a stable output voltage despite the fluctuation in load, which is fundamental to this research. An unstable output voltage reduces the design's efficiency and increases the dissipated power of the semiconductor electronic device. From this, the thermal performance of any power device is impacted. Consequently, the Peak Current Mode Control (CMC) strategy is considered in the design as it ensures the proper performance of the Flyback converter. The fundamental role of the CMC is to regulate the peak current in the inductor, provide the appropriate output power regulation, protect the circuit from any overcurrent, reduce output voltage ripple, and improve efficiency. A detailed explanation of the complete system design will be given in the following subtitles.

3.1.1 Flyback overview. The Flyback converter, one of the most widely used power supply topologies in power applications, is valued for its simplicity, cost-effectiveness, and versatile design. Unlike other power converters, the Flyback is known for efficiently isolating energy transfer between the transformer windings (Nambiar, Yahya, & Selvaduray, 2012). Moreover, it enables multiple output voltages from a single input source, enhancing its adaptability across various applications and making it a versatile and widely applicable design (C, Sreedevi, & Gopal, 2015).

3.1.2 Flyback converter: transfer of energy. Figure 5 below demonstrates a simple Flyback converter design done on QSPICE. It is a straightforward circuit consisting of an inductor, capacitor, diode, switch, resistor, and voltage source.

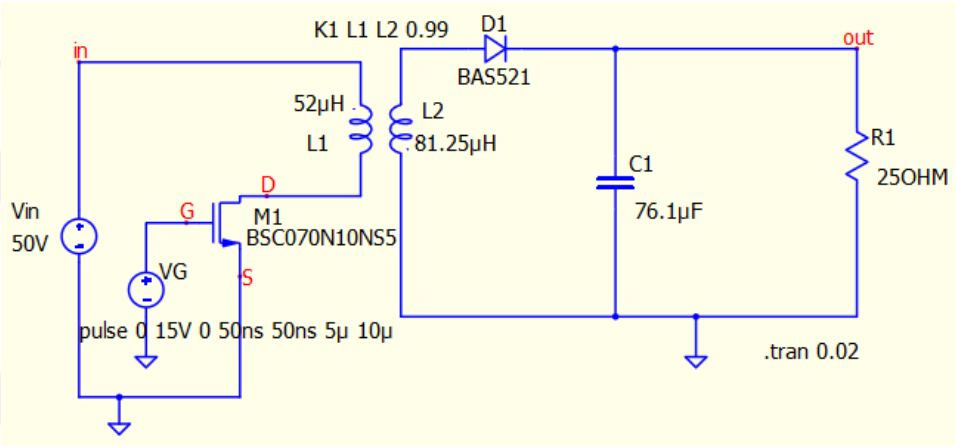

Figure 5. Basic flyback power converter design

The coupled inductors (L1, L2) in the above figure represent the primary and secondary sides of the transformer. When the Metal Oxide Semiconductor Field Effect Transistor (MOSFET) is ON (closed), energy is stored in the transformer's magnetic core as a magnetic field without transferring any power to the secondary side. The reason behind that is the reverse polarity of the transformer windings (see Figure 5), which leads to a reverse flow of current on the secondary side compared to the primary side. The catch Diode (D1) 's existence blocks the current flow when flowing in a reverse bias mode. At this period, the output capacitance (C1) delivers the load with energy. However, when the switch turns OFF (open), the sudden change in current reverses the polarity of the transformer windings, which puts the diode (D1) in the forward bias mode. In the meantime, the magnetic field stored in the transformer's magnetic core collapses, and the energy is transferred to the secondary side, which

supplies the load and charges the output capacitor (Nambiar, Yahya, & Selvaduray, 2012). The below equation gives the average output voltage (V_{out}).

$$V_{out} = \left(\frac{L_2}{L_1}\right)\left(\frac{D}{1-D}\right)V_{in}$$

, Where L_1& L_2 are the primary and secondary magnetic inductors, D is the duty cycle, and V_{in} is the input voltage.

Three main operation modes characterize the Flyback converter. Firstly, continuous conduction mode (CCM), where in this mode, the stored energy is not entirely transferred from the primary side to the secondary side when the switch is OFF (Halder, 2017) (Picard, 2010). This means that part of the stored energy remains in the transformer's primary winding when switching from OFF to ON. Secondly, discontinuous conduction mode (DCM) occurs when the switch is OFF during the complete transfer of energy from the primary to the secondary side (Load) of the transformer (Halder, 2017). This operation mode is known as the silent gap, where after the energy transfer is completed, no current flows in the primary side of the transformer before the beginning of the next cycle. Thirdly, the critical conduction mode (CRM), or transition mode (TM), is classified as between the CCM and DCM operation modes. It occurs when the stored energy is wholly dissipated and reaches zero at the end of the switching period (Picard, 2010). Figures 6, 7, and 8 below demonstrate a Flyback power converter's three main operation modes, explaining each's current flow when transitioning between ON and OFF states. In CCM operation, shown in Figure 6, the amount of power stored in the primary winding of a transformer is controlled by the switch, usually a MOSFET. When the switch is turned ON, denoted by $(D \times T_s)$ in Figure 6, the primary current Ip rises linearly to a peak current I_{pk} by a slope indicated as m_{1p}, which is determined by the input voltage and primary inductance. When the switch is turned OFF, denoted by $\left((1-D) \times T_s\right)$ in Figure 6, the primary current decreases as it transfers energy to the secondary winding, dropping to a minimum value of $I_{pk_{min}}$ before the next witching cycle. Simultaneously, the current at the secondary winding ramps up with a slope of m_{2S}, as energy is delivered to the output. Furthermore, the secondary current oscillates between its peak and minimum value, with an average of (I_{o-avg}) corresponding to the load current (Picard, 2010).

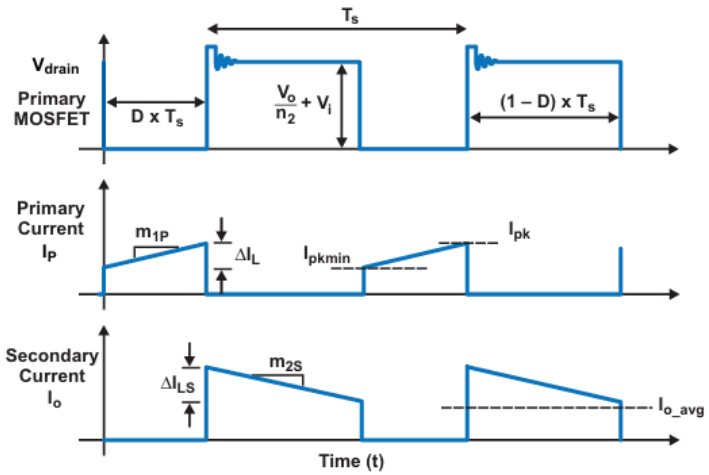

Figure 6. Operation in continuous conduction mode (CCM) (Picard, 2010)

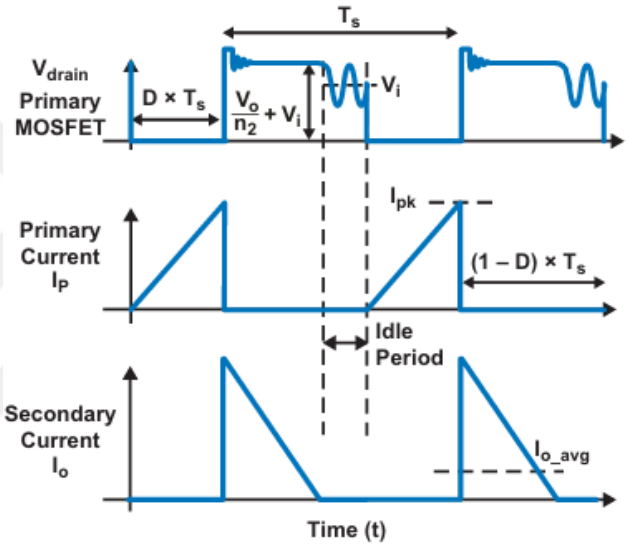

Figure 7. Operation in discontinuous conduction mode (DCM) (Picard, 2010)

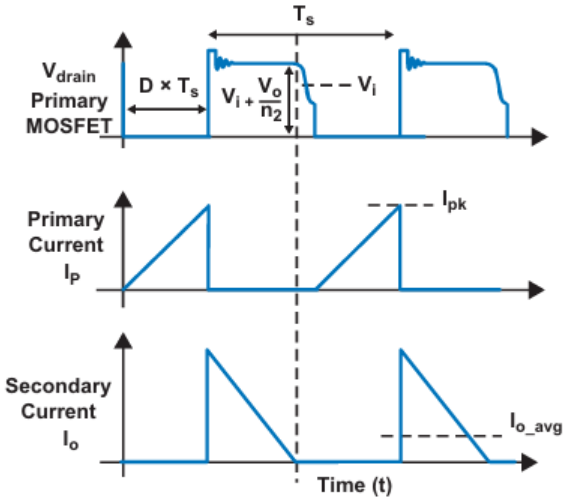

Figure 8. Operation in transition mode (TM) (Picard, 2010)

In DCM operation mode, shown in Figure 7, the primary current rises linearly when the switch (MOSFET) is ON from zero to a peak value that could be twice the current reached when operating at CCM mode. Additionally, the secondary current reaches zero before the end of each switching cycle when the MOSFET is turned OFF, resulting in an idle period where no current flows in the transformer. At this period, the voltage fluctuates around the input voltage (V_i) due to the absence of current. Unlike DCM, transition mode (TM) has no idle period, meaning energy is continuously transferred to the load. Moreover, the current in the primary winding begins to rise again as soon as the secondary current reaches zero as demonstrated in Figure 8 above.

3.1.3 Flyback converter: leakage inductance. Leakage inductance measures the energy stored in the magnetic field generated by a winding but does not couple to the other winding. The current flow in a Flyback transformer is unique due to its superior isolation property. It is designed to completely isolate the energy from transferring from the primary to the secondary side when the switch (MOSFET) is ON. As a result of the current flowing in the primary side, magnetic energy is built up in the transformer coil. When the switch is OFF, the magnetic energy transfers from the primary to the secondary side, delivering it to the load. However, not all the stored energy is efficiently transferred to the secondary winding due to the leakage inductance. Part of the magnetic flux initiated by the primary side of the transformer doesn't link with the secondary transformer winding, leading to a leakage. Instead, it is concentrated near the primary side due to the failure to transfer energy (Kewei et al., 2009). This leakage energy is harmful to the system and primarily unfavourable as it doesn't contribute to energy transfer. Yet, it can cause high voltage spikes and stress on the circuit components. Moreover, leakage inductance reduces the system's efficiency, causes a loss of volts-seconds during switching, and generates electromagnetic interference (EMI). The stored energy in a transformer leakage inductance has no path to smoothly dissipate, resulting in oscillations. To avoid such matters, a clamp and RC snubber circuits are considered in this design to protect the design components while maintaining the best performance and efficiency with minimum loss.

3.1.4 Flyback converter: clamp and RC snubber. To maintain an efficient and stable system, it is crucial to ensure the durability and reliability of design

components. The high voltage spikes and ringing caused by the leakage inductance are harmful and could cause stress on the device components. Therefore, using the snubber and clamp circuit greatly protects and optimizes the circuit. As its name indicates, the RC snubber circuit consists of a resistor and a capacitor connected in series, as shown in Figure 9 below. These components are connected regularly in parallel to the MOSFET used at the primary side of the transformer. RC snubber circuit is intended to mitigate or absorb undesirable transient voltages and currents that arise from inductive or capacitive loads and fast switching actions. Moreover, it reduces the voltage ringing caused by the transformer leakage inductance and parasitic capacitance (Kanthimathi & Kamala, 2015).

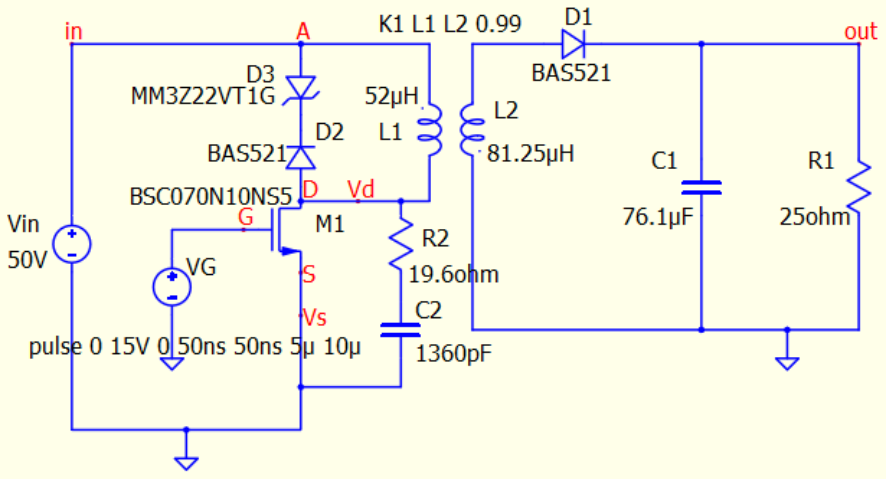

Figure 9. Flyback converter design with RC snubber and clamp circuit

The resistor (R2) role dissipates energy from the oscillations, reducing their amplitude over time and damping the oscillatory behaviour. On the other hand, the capacitor (C2) paves a smooth path for the leakage inductance energy, reducing the transient time that allows the resistor (R2) to dissipate the stored energy as heat. This ensures the stabilizing of the circuit voltage and the reduction of the high voltage spike in the MOSFET. Furthermore, the clamp circuit consists of a diode and a Zener diode connected in series together and both in parallel to the primary winding of the transformer. The purpose of the clamp circuit is to restrict the peak voltage across the MOSFET switch by limiting the voltage spike to a specific level. In normal operating conditions, both diodes remain off until a voltage spike occurs due to the switch turning OFF. The standard diode is the forward bias direction and conducts in this case. This creates a path for the excess current to run away from the circuit-sensitive

components. The Zener diode is designed to perform in a reverse-biased direction when the voltage applied to it exceeds its breakdown voltage, contributing to clamping the voltage to the specified Zener voltage level. RC snubber and clamp circuit tends to protect the sensitive components of a circuit design. However, one of their disadvantages is that they reduce the design's efficiency due to the vast amount of dissipated power, which is considered lost. Therefore, the need for such circuits should be carefully evaluated based on the design criteria and objectives (Kanthimathi & Kamala, 2015) (Picard, 2010).

3.1.5 Flyback converter: Peak Current Mode Control (CMC). Current mode control has been widely recognized as an effective and practical method for improving the performance of pulse width modulated (PWM) switching power converters. Load variations significantly impact the output voltage regulation, overall system efficiency, and design stability. Therefore, the peak current mode strategy controls and regulates the power supply's output voltage, maintaining its strength and reliability even if the current drawn is increased. Unlike Voltage mode control (VCM), CMC consists of two feedback loops: one inner current loop and one outer voltage loop (Yang, 2016). Figure 10 below demonstrates the complete design of the Flyback converter with the Peak current mode control methodology.

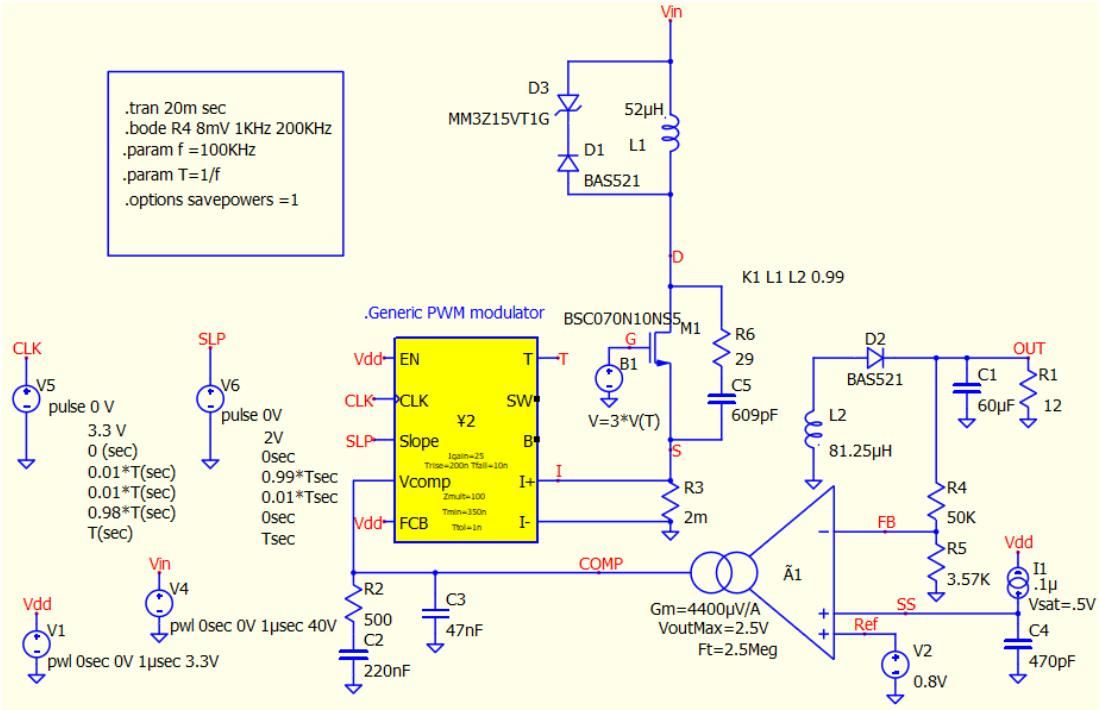

Figure 10. Flyback converter circuit design with Peak current mode control

One of the most significant challenges researchers face when simulating a DC-DC converter is the absence of the controller IC. A practical solution involves utilizing a discrete PWM modulator, often implemented using an SR latch, as a substitute for the specific controller IC model. In this context, QSPICE offers a generic and easy-to-use SMPS flip flop that can be utilized to model any switch-mode power supply controller. Furthermore, QSPICE is fast, making it ideal for evaluating various component parameters in designs operating at a 100KHz switching frequency or even higher. The key aspects covered in this section include demonstrating the role of the CMC in regulating the output voltage while maintaining high efficiency. On the other hand, the phenomenon of subharmonic oscillations in current mode control is illustrated, along with highlighting the effective technique for implementing the slope compensation to limit and dampen these oscillations. In addition, the soft starter technique's role is to protect the MOSFET against high voltage spikes. The current source (I_1) gradually ramps the voltage during start-up, charging the capacitor. As a result, the stress on the device is reduced, mitigating any disturbance in its characteristics (Shetty & Kumar, 2017).

The process starts with the outer voltage loop sensing the output voltage at each switching cycle. To achieve this, the output voltage is scaled down using a voltage divider, formed by R_4 & R_5, positioned at the output side to bring Vout to a level close to the reference voltage (V_{ref}). This voltage is called the feedback voltage (V_{fb}). V_{fb} is taken as an input at the inverting terminal and compared with the inputs at the non-inverting terminals of the transconductance amplifier (Gm amplifier). Figure 10 demonstrates the Gm amplifier having two non-inverting input terminals: a reference voltage of 0.8V and a soft starting ramp voltage. The decision of the reference voltage value depends on each circuit design. Referring to the datasheets of adjustable frequency current mode Flyback controllers, for example, the LTC3805-5, it is specified that the transconductance amplifier operates with a feedback voltage range between 0.78 V and 0.812 V. Up on this, the reference voltage is taken at 0.8 V (Analog Devices, 2024). The voltage divider resistor values are calculated as shown below:

$$V_{Reference} = \frac{V_{out} * R_5}{R_4 + R_5}$$

$$0.8 = \frac{12 * R_5}{R_4 + R_5}$$

Assuming $R_4 = 50K$, then the value of R5 is:

$$0.0667 = \frac{R_5}{50k + R_5}$$

$$R_5 = 3.57k\Omega$$

Additionally, the current source I_1 and the capacitor (C_4) in the above design represent the soft starting strategy, considered the second non-inverting input of the Gm amplifier. The current source supplies the capacitor with constant current, resulting in a linear voltage increase across the capacitor. In every switching cycle, the feedback voltage is compared with both voltages, the reference voltage V_{fb} and the soft starting voltage (V_{ss}) . Initially, with the circuit being off, the feedback voltage is zero. As the soft starter voltage increases, both V_{fb} and V_{ss} remain close to zero compared to V_{ref} . Subsequently, both V_{ss} and V_{fb} increase linearly until the feedback voltage approaches 0.8V. At this point, V_{ss} continues to increase linearly, while the feedback voltage will saturate close to V_{ref} throughout the rest of the period. This occurs because the difference between V_{fb} and V_{ref} becomes smaller than between V_{fb} and V_{ss}. The Gm amplifier is designed to generate an output current proportional to the difference between the two voltages. Mathematically, for every 1 volt of difference, it produces an output current of 4400 μA. This current is often used to charge/discharge a capacitor in the compensation network, which is employed to assess the system's stability. In this design, the compensation network consists of Resistor (R_2) and capacitors (C_2) and (C_3). The command ". bode R4 8M 100 200K", shown in Figure 10, is used to simulate an open loop frequency response of the SMPS. This command applies a small signal of 8mV on the R4 resistor and sweeps the frequency from 1KHz to 200KHz to measure the loop gain and phase. Inductors and capacitors introduce phase shifts in the system, leading to positive feedback and causing the design to become unstable. The compensation network controls this phase shift and ensures a stable design by providing negative feedback.

The process continues when the inner current loops sense the current across the sensing resistor ($2\ m\Omega$ in this design). The generic PWM modulator (Y_2) shown in the circuit takes in the sensed current and the compensation voltage. Moreover, the clock

signal (CLK) is a pulse signal that ensures the circuit operates under a fixed switching frequency. For simplification purposes, the rise time, fall time, and ON time were subject to the change in the switching frequency. The clock signal duty cycle was set to be 98%. In addition, the slope compensation signal (SLP) stabilizes the current loop to prevent unneeded oscillations.

3.1.6 Flyback converter: slope compensation. Slope compensation is an artificial ramp signal generated by an RC network and added to the sensed inductor current. The use of a slope compensation circuit is decided if three main conditions are met: operating under fixed switching frequency, duty cycle higher than 50%, and using a Peak current mode control strategy. Such a critical network can prevent subharmonic oscillations when the duty cycle is near, reaches, or exceeds 50%, ensuring the proper operation of the design. Furthermore, the sensed inductor current is scaled by the current gain and combined with the slope compensation voltage (V_{Comp}). When the resulting voltage reaches the compensation voltage (V_{Comp}), the MOSFET is turned OFF until the beginning of the next cycle. The output signal of the generic PWM modulator is amplified by a factor of three to achieve the required level for controlling the MOSFET.

3.2 Data Collection Instruments

QSPICE is the latest generation of SPICE simulation software developed and launched by Analog Devices in June 2023. QSPICE is very fast, making it the best choice for engineers to use when modeling complex circuits. Moreover, it's an open source that can be reached by anyone and is easy to deal with. Lastly, it supports coding languages where C++ and Verilog can be integrated into the software for component and signal modeling.

3.3 Data Collection Procedure

- Use the circuit designed in section 3.1.6.
- Run a transient time-domain analysis of 20 ms (millisecond).
- Click on the node (out) to plot the output voltage and on the node (Vin) for the input voltage.
- Click on node D to plot the drain to source voltage and record the value.

- Hold CTRL and click on the load R1 to measure the output power dissipation.
- Repeat the same for the input voltage Vin to plot its power dissipation
- In the simulation window, zoom in on the last 15 ms of the simulation to ensure that only the steady-state values are used in the calculations.
- Right-click on the data label and select "average."
- Divide the average output power by the average input power to calculate efficiency and record the result in the table.
- Hold CTRL and click on the MOSFET to measure its power dissipation.
- Record the average steady-state power dissipation of the MOSFET in the table.
- Use this dissipation value to calculate the new operating temperature.
- Divide the value by 12 W (the output power of the power supply) to calculate the transistor's effect on the system's overall efficiency as a percentage.
- Change the transistor and repeat the data collection procedure.
- Change the switching frequency and repeat the data collection procedure
- Change the input voltage and repeat the data collection procedure

Table 6

Chosen Semiconductor Power Devices From Qspice Simulation

S. N	Device part no.	Type	Manufacturer	Vds[V]	Ids[A]	Rds-on [mΩ]	Qg [nC]
1	BSC070N10NS5	Si	Infineon	100	80	6	41
2	SQ3426EEV	Si	Vishay	60	7	57	7.6
3	BSC123N08NS3	Si	Infineon	80	55	12.3	19
4	FTA07N60	Si	ARK Microelec.	600	7	900	38.6
5	EPC2218	GaN	EPC	100	60	2.4	10.5
6	GS66508B	GaN	GaN Systems	650	30	50	6.1
7	GS66516T	GaN	GaN Systems	650	60	25	14.2
8	UF3C065040	SiC	Qorvo	650	41	42	51
9	UF3C065080	SiC	Qorvo	650	25	80	51
10	UJ4C075023	SiC	Qorvo	750	66	23	37.8
11	UF3C120040	SiC	Qorvo	1200	65	35	51
12	UF3C120080	SiC	Qorvo	1200	21	85	23
13	UF3C170400	SiC	Qorvo	1700	8	410	27

QSPICE provides many different electronic semiconductor devices made of various materials, such as Silicon (Si), Silicon Carbide (SiC), and Gallium Nitride (GaN). Table 6 above demonstrates the different MOSFETs in the QSPICE library chosen in this study.

3.4 Data analysis procedure

First, data must be segregated based on the switching frequency, input voltage, and semiconductor material. Then, bar charts will be used to visualize the data, making it easy to compare the transistor's efficiency and performance under different operating conditions.

3.5 Limitation

QSPICE is an analytical and simulation tool used in microelectronics that is limited in its ability to model real-world applications. It is easier said than done to control such parameters as the temperature difference levels or the worn-out devices. However, the QSPICE library contained fewer numbers of Si and GaN MOSFET models than that of SiC MOSFET models. This limited me from conducting a broader comparison and accumulating other data from various types of MOSFETs.

Chapter 4

Findings

In this section, simulation results will be conducted to evaluate and differentiate the performance of each semiconductor material in a Flyback power converter. Firstly, simulations will be implemented on a Flyback converter with an RC snubber and clamp circuits under various operating conditions. Secondly, the effect of removing these circuits on the design will be tested under the same conditions. This section will show the impact of changing either the input voltage or switching frequency on the performance of the semiconductor device.

4.1 Flyback Converter With RC Snubber and Clamp Circuit

Firstly, the input voltage V_{in} is set to 40V and the switching frequency is set to 100KHz. Secondly, the switching frequency will be increased to 200KHz while maintaining the input voltage constant at 40V. The input voltage will be increased to 100V, and a simulation test will be implemented when the switching frequency is 100KHz and 200KHz.

4.1.1 Silicon-type MOSFETs. Figure 11 below illustrates a Flyback converter's input and output voltage for a Si-type MOSFET (BCS070N10NS5). It can be seen that the output voltage was recorded to be 12 V as planned. Moreover, Figure 12 below demonstrates the drain to source voltage (V_{ds}) of the chosen silicon mosfet with a maximum value of around 60V. Furthermore, Figure 13 below shows the simulation results of the average instantaneous output power at the load side (R_1) and the average instantaneous input power at the power supply. The output power has measured an average of 12.0096 W. In contrast, the input power recorded an average of 14.5765 W. Therefore, the efficiency of the circuit using a silicon mosfet (BCS070N10NS5) was calculated as shown below:

$$Efficiency = \frac{Pout - avg.}{Pin - avg.} \times 100\% = \frac{12.0096}{14.5765} = 82.4\%$$

Regarding power dissipation, Figure 14 below illustrates a zoomed simulation result of the silicon MOSFET's instantaneous power dissipation when operating under the defined operating conditions. It was recorded that the silicon MOSFET had an average value of 0.0867475 W.

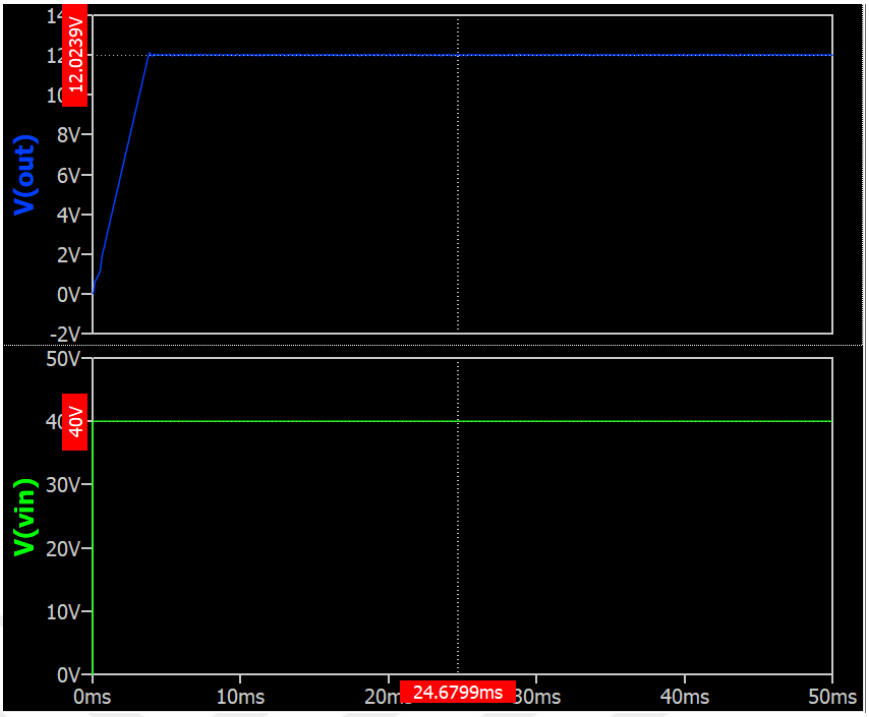

Figure 11. Input voltage (V_{in}) vs. output voltage (V_{out}) for silicon mosfet

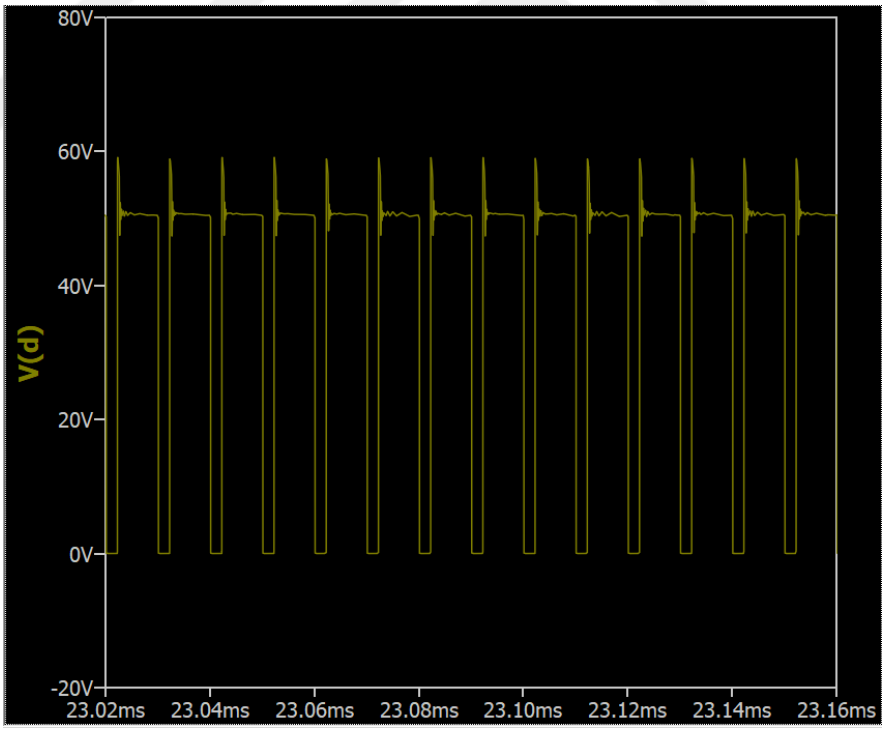

Figure 12. Silicon mosfet drain to source voltage

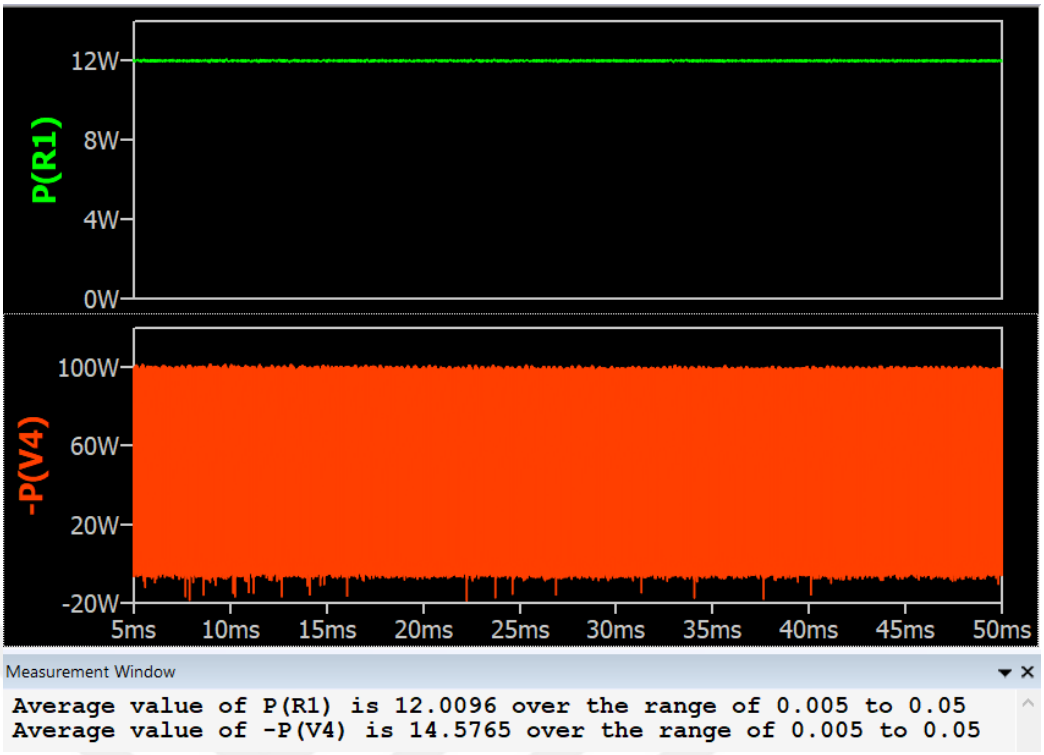

Figure 13. Average output power vs average input power of silicon mosfet

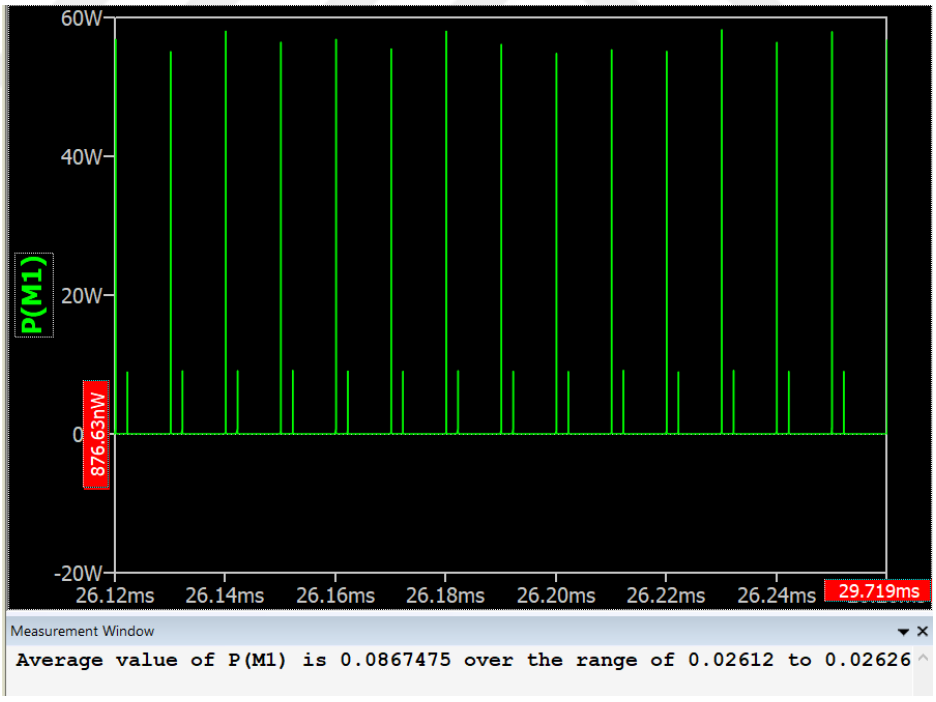

Figure 14. Instantaneous power dissipation of silicon mosfet

Additionally, Thermal management could be calculated using the average power dissipation value obtained. The BCS070N10NS5 MOSFET datasheet shows that the

junction-to-case thermal resistance (R_{thJC}) is 1.5 K/W. At the initial stage, any electronic device's operating temperature (T_j) is around 27°, corresponding to a room temperature. Therefore, the new operating temperature of the MOSFET is calculated as follows:

$$New\ temp. = (R_{thJC} * P_{M1-avg}) + T_J = (1.5 * 0.0867475) + 27° = 27.13°$$

The market unit price for the MOSFET mentioned above is around 0.82€. The prices were considered for various devices as the economic aspect is crucial to assess. The same tests were done on different Si MOSFETs to study and evaluate the performance of silicon power devices with other characteristics and properties. The results are shown in Tables 7, 8, and 9 below.

Table 7

Simulation Results of Silicon Mosfets Operating at Vds= 40V, Fs= 100KHz

Device Part no.	Output voltage(V)	Drain voltage(V)	Efficiency (%)	Power Diss. (W)	Temp. (°C)	P.D in %
BSC070N10NS5	12	Max. 60V	82.4%	0.086747	27.13	0.5712
SQ3426EEV	12	Max. 60V	81.59%	0.07375	27.31	0.6145
BSC123N08NS3	12	Max. 60V	82.17%	0.068546	27.13	0.5712
FTA07N60	12	Max. 60V	78%	0.754402	30	6.2866

Table 8

Simulation Results of Silicon Mosfets Operating at Vds=40V, Fs= 200KHz

Device Part no.	Output voltage(V)	Max. Drain voltage(V)	Efficiency (%)	Power Diss. (W)	Temp. (°C)	P.D in %
BSC070N10NS5	12	60V	79.70%	0.17013	27.26	1.418
SQ3426EEV	12	60 V	79.50%	0.11662	27.49	0.972
BSC123N08NS3	12	60V	79.7%	0.1309	27.25	1.091
FTA07N60	12	60V	76%	0.8338	30.34	6.948

Table 9

Simulation Results of Silicon Mosfet Operating at Vds=100V, Fs= 100KHz & Fs= 200KHz

Freq. (Hz)	Device Model	Vout (V)	Drain Voltage (V)	Eff. (%)	Power Diss. (W)	Temp. (°C)	P.D (%)
100KHz	FTA07N60	12	120V	77%	0.67	29.68	5.58
200KHz	FTA07N60	12	120V	71.5%	1.167	31.67	9.72

4.1.2 Gallium Nitride (GaN) MOSFETs

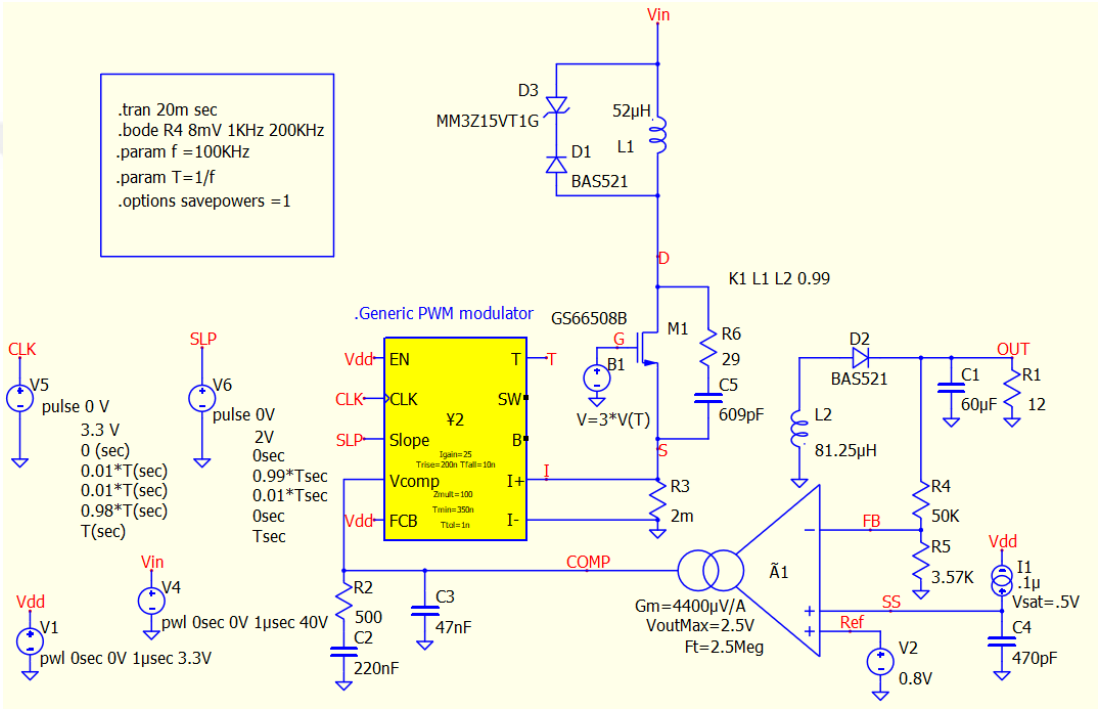

Figure 15. Flyback power converter using GaN MOSFET

Figure 15 above demonstrates the Flyback design with a GaN MOSFET device type GS66508B. Furthermore, Figure 16 below shows the output voltage of the designed circuit observed to be 12V, as expected.

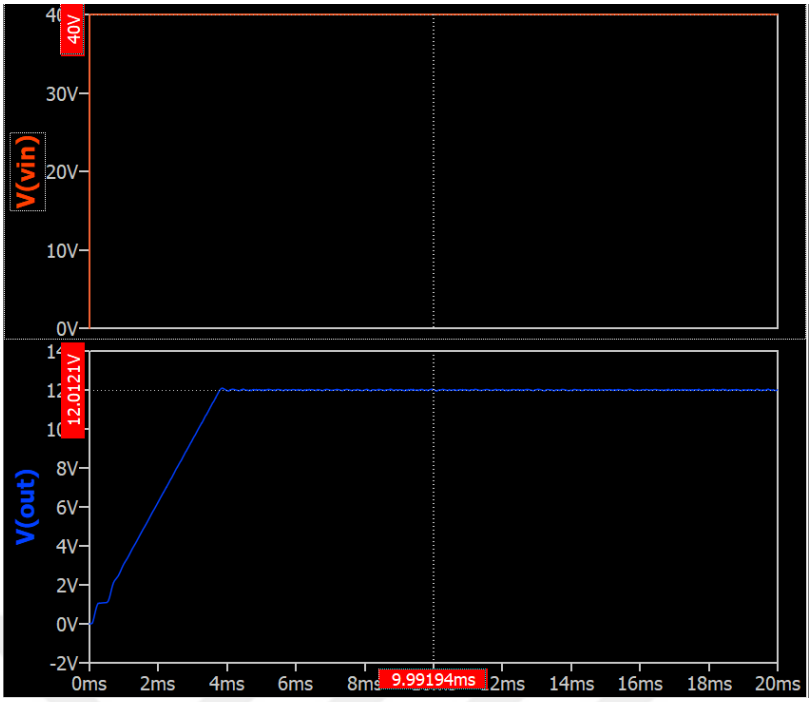

Figure 16. Input voltage vs. output voltage of GaN MOSFET

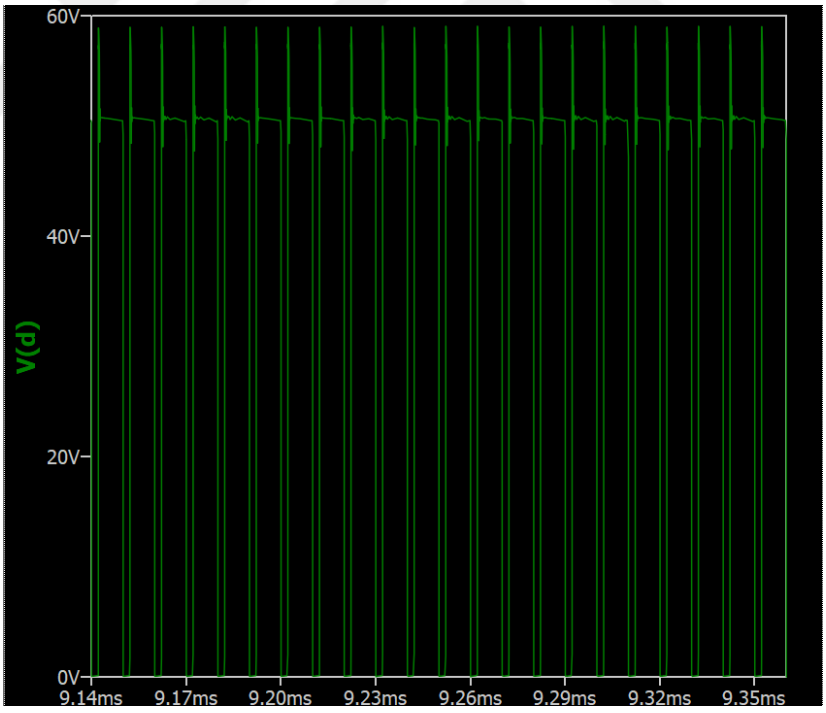

Figure 17. Drain to source voltage of GaN MOSFET

Figure 17 above represents the drain-to-source voltage across the GaN MOSFET, where the maximum voltage was recorded to be approximately 60V. Furthermore, Figure 18 below illustrates the output power at the load side (R1) and the

input power at the power supply. The output power has recorded an average of 12.0098W. In contrast, the input power recorded an average of 14.6583 W. Therefore, the efficiency of the circuit using a GaN mosfet (GS66508B) was calculated as shown below:

$$Efficiency = \frac{Pout - avg.}{Pin - avg.} \times 100\% = \frac{12.0098}{14.6583} = 82\%$$

Regarding power dissipation, Figure 19 below depicts the simulation plot of the GaN MOSFET's instantaneous power dissipation. It can be seen that the MOSFET had an average value of 0.0499413 W. Upon this, the effect of power dissipation on the GaN MOSFET temperature when operating is as shown:

$$New\ temp. = (R_{thJC} * P_{M1-avg}) + T_J = (0.5 * 0.0499413) + 27° = 27.025°$$

Additionally, the market unit price for the GaN MOSFET mentioned above is around 17.1 €.

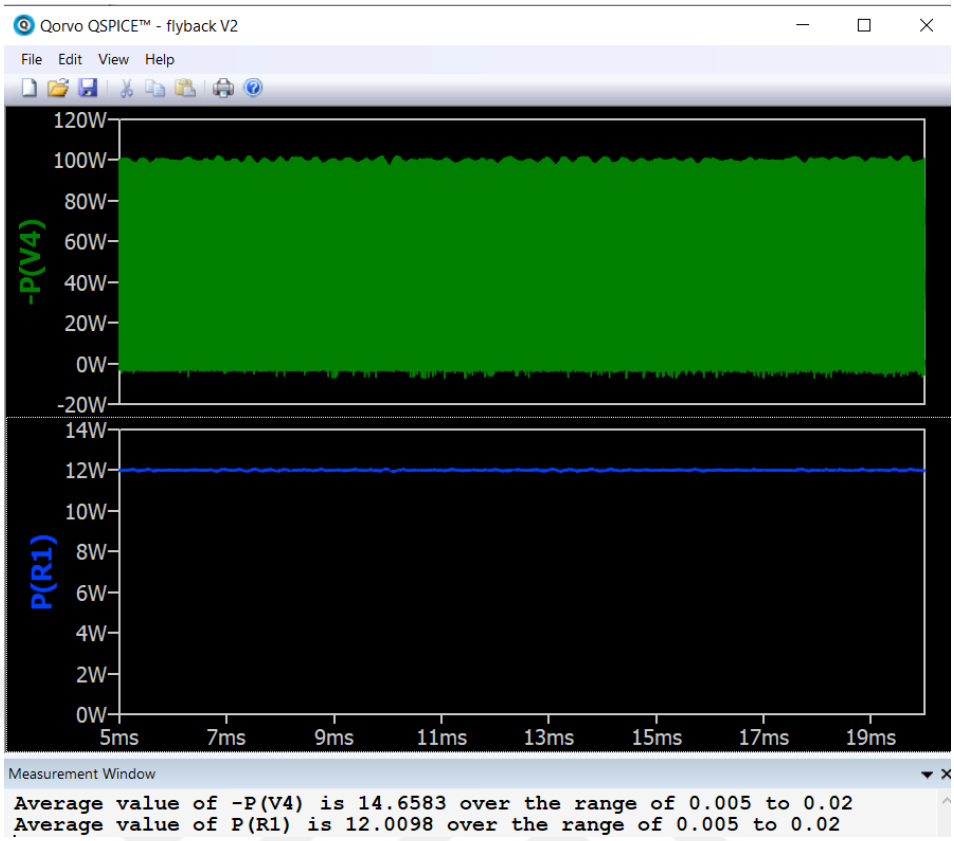

Figure 18. Average output power vs average input power of GaN mosfet

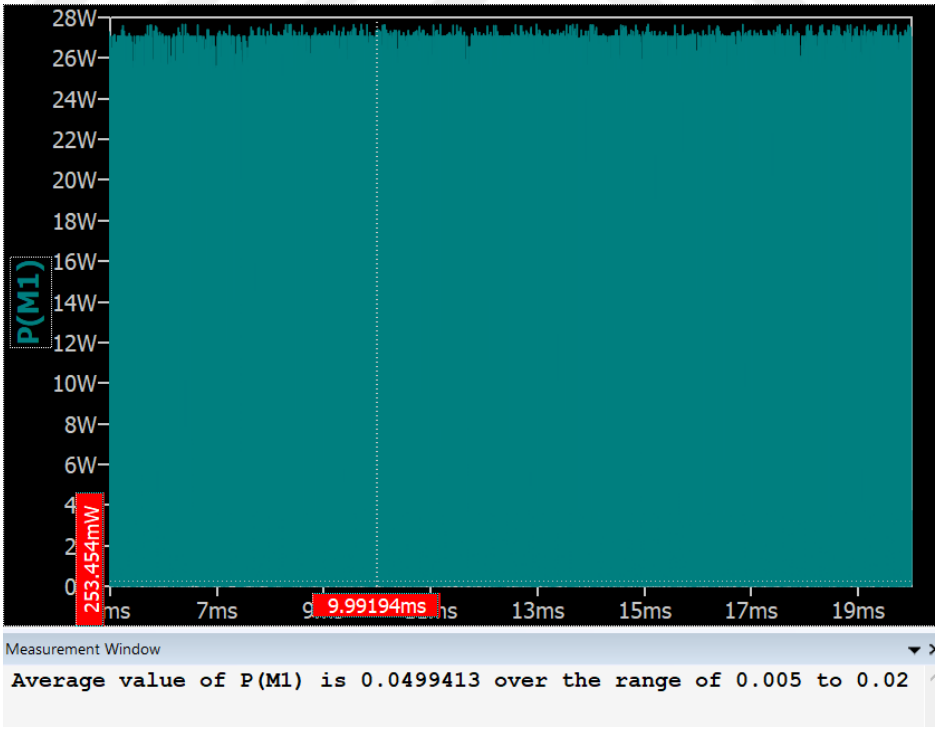

Figure 19. Instantaneous power dissipation of GaN mosfet

Tables 10, 11, 12, and 13 below present the simulation results implemented on available GaN MOSFETs. They list the efficiency, power dissipation, output voltage, drain voltage, and operating temperature of the chosen GaN power devices, which depicts the performance of GaN power MOSFETs under different operating conditions, such as increasing either the input voltage or the switching frequency.

Table 10

Simulation Results of GaN MOSFETs Operating at Vds= 40V, Fs= 100KHz

Device Part no.	Output voltage(V)	Max. Drain voltage(V)	Efficiency (%)	Power Diss. (W)	Temp. (°C)	P.D (%)
EPC2218	12	App. 60 V	82.70%	0.0472	27.02	0.3932
GS66508B	12	App. 60 V	82%	0.05	27.025	0.41
GS66516T	12	App. 60V	82.2%	0.0521	27.01	0.4338

Table 11

Simulation Results of GaN Mosfets Operating at Vds= 40V, Fs= 200KHz

Device Part no.	Output voltage (V)	Max. Drain voltage(V)	Efficiency (%)	Power Diss. (W)	Temp. (°C)	P.D (%)
EPC2218	12	App. 60 V	79.70%	0.0931	27.05	0.7760
GS66508B	12	App. 60 V	79.50%	0.0647	27.03	0.5394
GS66516T	12	App. 60 V	79.7%	0.0824	27.02	0.6864

Table 12

Simulation Results of GaN Mosfets Operating at Vds= 100V, Fs= 100KHz

Device Part no.	Output voltage (V)	Max. Drain voltage(V)	Efficiency (%)	Power Diss. (W)	Temp. (°C)	P.D (%)
GS66508B	12	App. 120V	78.80%	0.0857441	27.043	0.715
GS66516T	12	App. 120V	79.2%	0.127918	27.034	1.066

Table 13

Simulation Results of GaN Mosfets Operating at Vds= 100V, Fs= 200kHz

Device Part no.	Output voltage (V)	Max. Drain voltage(V)	Efficiency (%)	Power Diss. (W)	Temp. (°C)	P.D (%)
GS66508B	12	App. 120V	73.80%	0.151226	27.08	1.260
GS66516T	12	App. 120V	73.5%	0.244696	27.07	2.039

4.1.3 Silicon Carbide-Type MOSFET

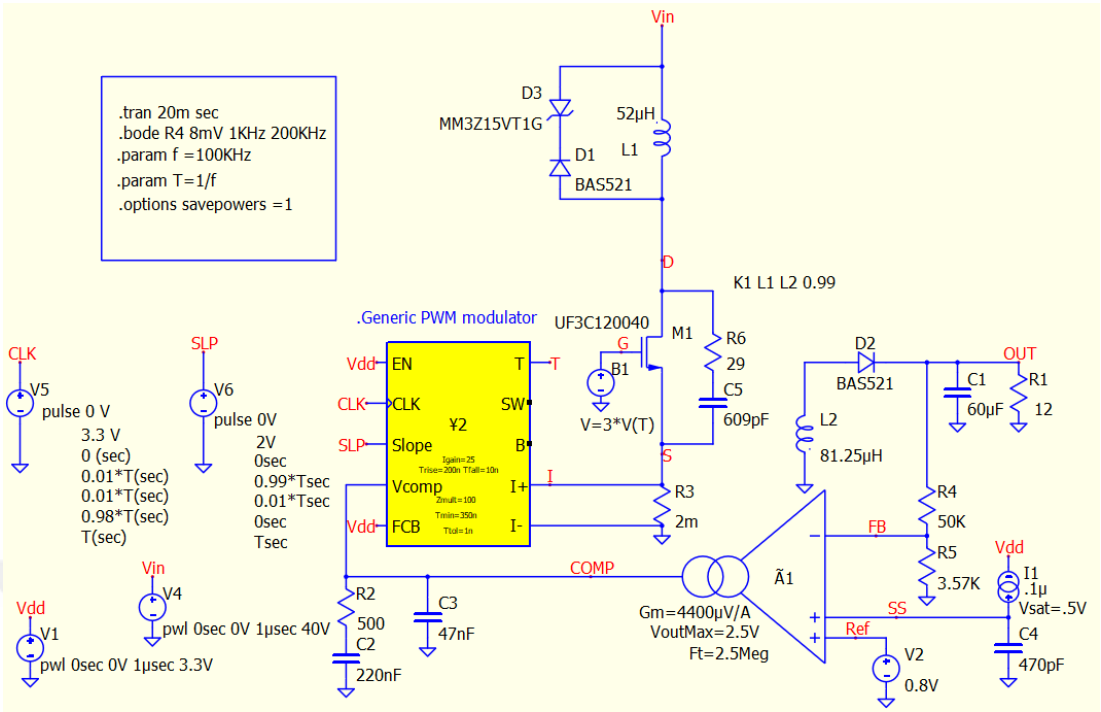

Figure 20. Flyback power converter using SiC MOSFET

Figure 20 above presents the Flyback converter power supply with Silicon Carbide (SiC) MOSFET type UF3C065030. Furthermore, Figure 21 below demonstrates the performance of SiC MOSFET in the circuit design under a fixed input voltage of 40 V and a fixed switching frequency of 100KHz. The instantaneous input power recorded an average of 14.5339 W, where the instantaneous output power recorded an average of 12.0091 W. Upon this, the efficiency of the design is calculated to be 82.6%, and the new junction-to-case temperature of the MOSFET is calculated to be 27.16 degrees, as shown in the equations below.

$$Efficiency = \frac{Pout - avg.}{Pin - avg.} \times 100\% = \frac{12.0091}{14.5339} = 82.6\%$$

$$New\ temp. = (R_{thJC} * P_{M1-avg}) + T_J = (0.34 * 0.490521) + 27° = 27.16°$$

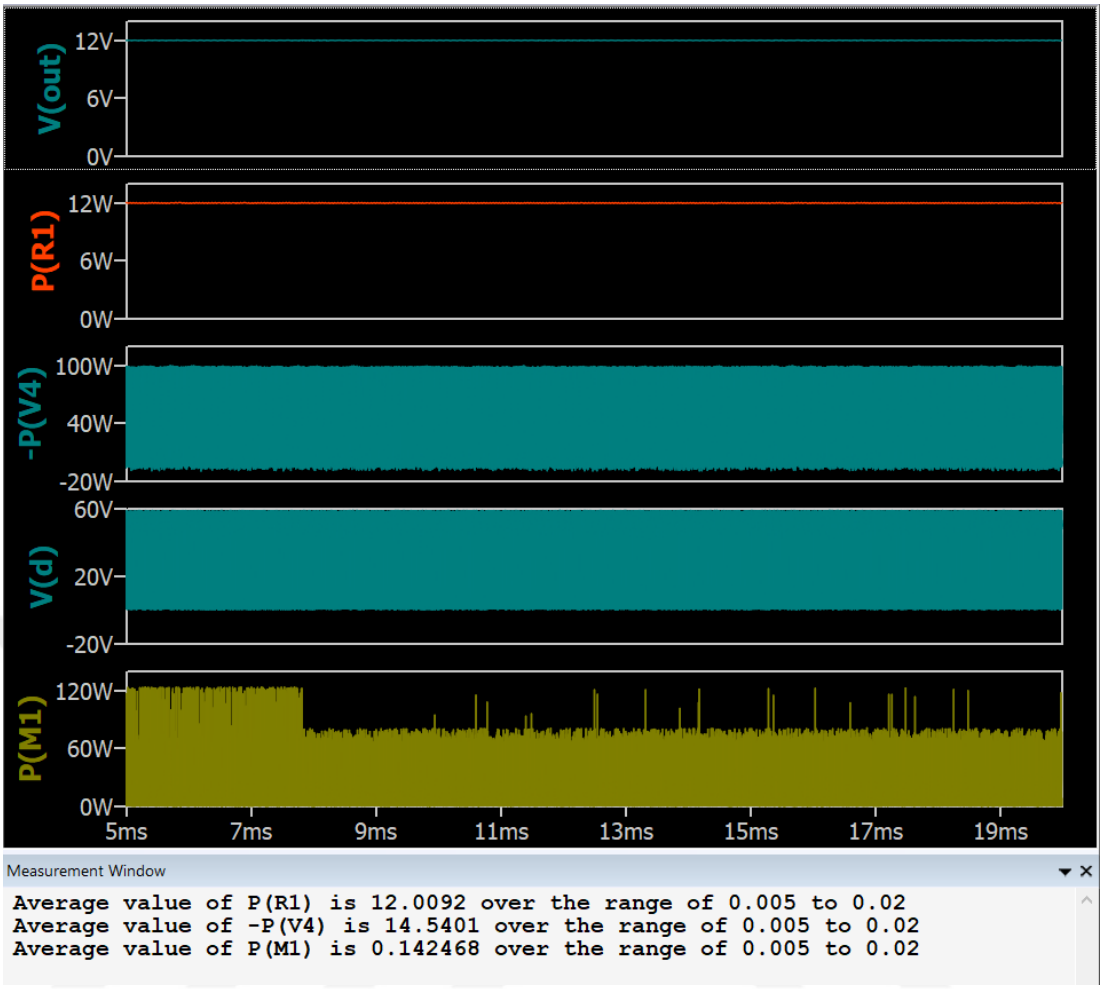

Figure 21. SiC MOSFET instantaneous output power (P(R1)), instantaneous input power (P_{V4}), MOSFET dissipated power (P_{M1}), drain voltage (V_d), and output voltage (V_{out}), (up to down)

Tables 14, 15, 16, and 17 below demonstrate the simulation results of different SiC MOSFETS under different operating conditions.

Table 14

Simulation Results of SiC Mosfets Operating at Vds= 40V, Fs= 100KHz

Device Part no.	Output voltage(V)	Max. Drain voltage(V)	Efficiency (%)	Power Diss. (W)	Temp. (°C)	P.D (%)
UF3C065080	12	App. 60 V	81.60%	0.121	27.133	1.008
UF3C065040	12	App. 60 V	82.4%	0.127	27.05	1.060
UJ4C075023	12	App. 60 V	82.8%	0.112	27.05	0.931
UF3C120040	12	App. 60 V	82.6%	0.143	27.05	1.187
UF3C120080	12	App.60 V	82.3%	0.117	27.05	0.975
UF3C170400	12	App. 60 V	80.20%	0.321	27.5	2.674

Table 15

Simulation Results of SiC Mosfets Operating at Vds= 40V, Fs= 200KHz

Device Part no.	Output voltage(V)	Max. Drain voltage(V)	Efficiency (%)	Power Diss. (W)	Temp. (°C)	P.D (%)
UF3C065080	12	App. 60 V	79.2%	0.19	27.21	1.58
UF3C065040	12	App. 60 V	80%	0.228	27.10	1.90
UJ4C075023	12	App. 60 V	79.6%	0.220	27.11	1.84
UF3C120040	12	App. 60 V	79.4%	0.274	27.10	2.28
UF3C120080	12	App. 60 V	80%	0.164	27.13	1.37
UF3C170400	12	App. 60 V	78.13%	0.350	27.52	2.917

Table 16

Simulation Results of SiC Mosfets Operating at Vds= 100V, Fs= 100KHz

Device Part no.	Output voltage(V)	Max. Drain voltage(V)	Efficiency (%)	Power Diss. (W)	Temp. (°C)	P.D (%)
UF3C065080	`12	App. 120 V	78.75%	0.238	27.262	1.98
UF3C065040	12	App. 120 V	79.1%	0.321	27.15	2.67
UJ4C075023	12	App. 120 V	79.2%	0.346	27.17	2.88
UF3C120040	12	App. 120 V	78.8%	0.349	27.12	2.91
UF3C120080	12	App. 120 V	79%	0.225	27.18	1.87
UF3C170400	12	App. 120 V	77.70%	0.263	27.39	2.19

Table 17

Simulation Results of SiC Mosfets Operating at Vds=100V, Fs= 200KHz

Device Part no.	Output voltage(V)	Max. Drain voltage(V)	Efficiency (%)	Power Diss. (W)	Temp. (°C)	P.D (%)
UF3C065080	12	App. 120 V	73.8%	0.47602	27.524	3.97
UF3C065040	12	App. 120 V	73.70%	0.6679	27.31	5.56
UJ4C075023	12	App. 120 V	73.4%	0.706	27.34	5.88
UF3C120040	12	App. 120 V	73.2%	0.754	27.26	6.28
UF3C120080	12	App. 120 V	74.0%	0.420	27.3	3.50
UF3C170400	12	App. 120 V	73.18%	0.424	27.64	3.53

4.1.4 Si, GaN, & SiC overall comparison

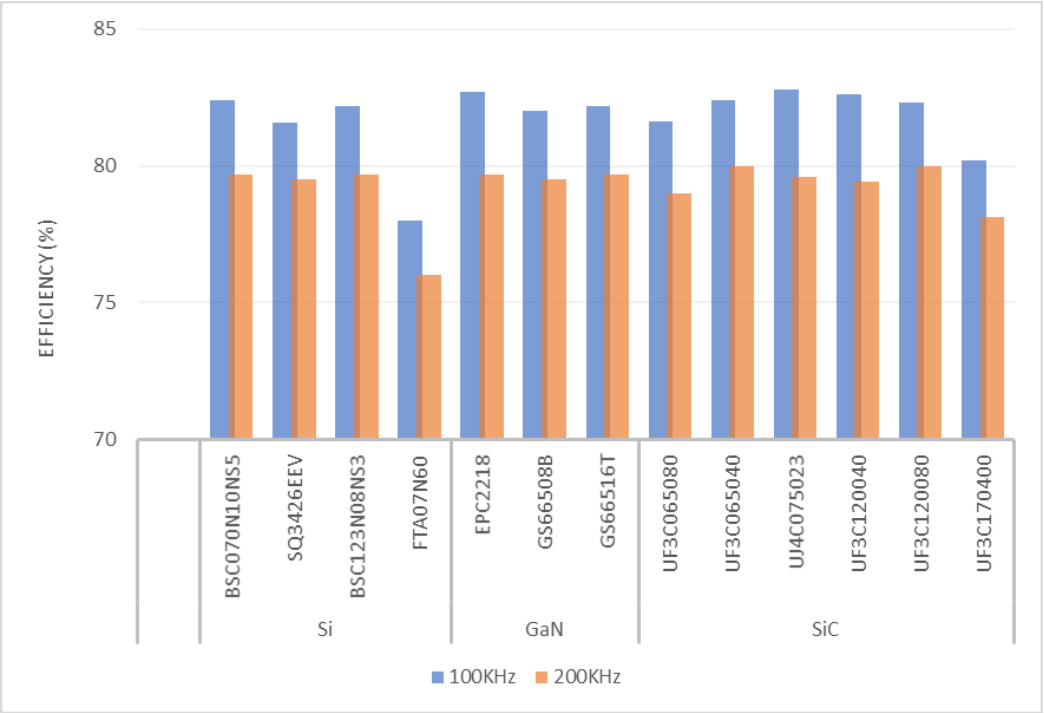

Figure 22. Efficiency plot of Si, GaN, & SiC devices operating at Vds= 40V

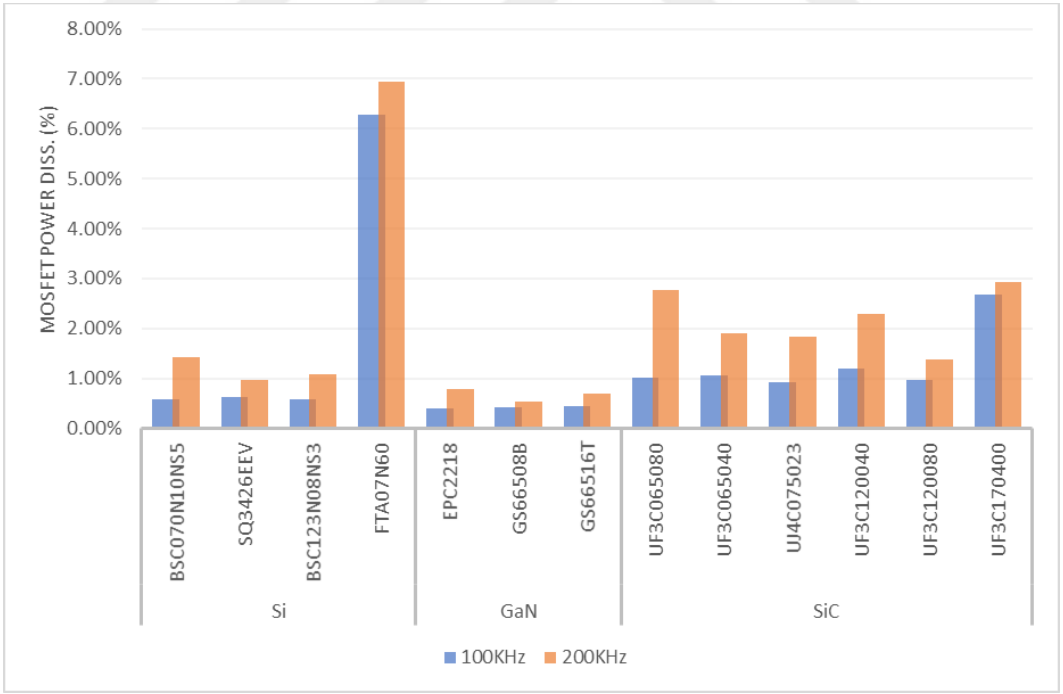

Figure 23. Effect of MOSFET power dissipation on efficiency, operating @40V

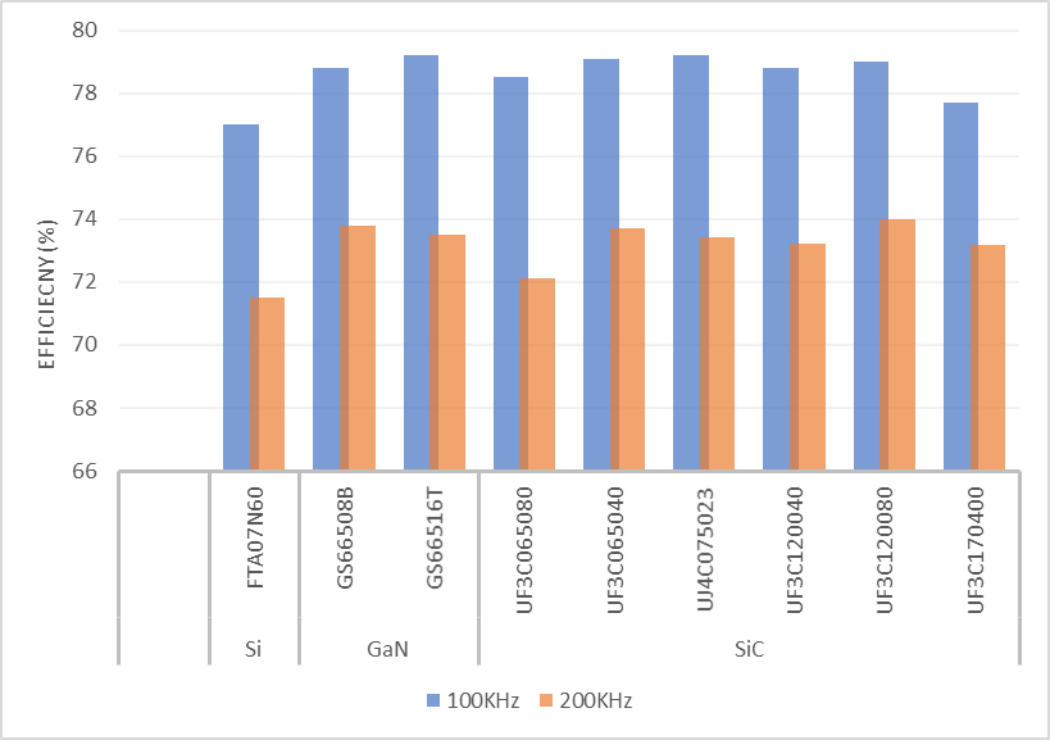

*Figure 24.*Efficiency plot of Si, GaN, & SiC devices operating at Vds= 100V

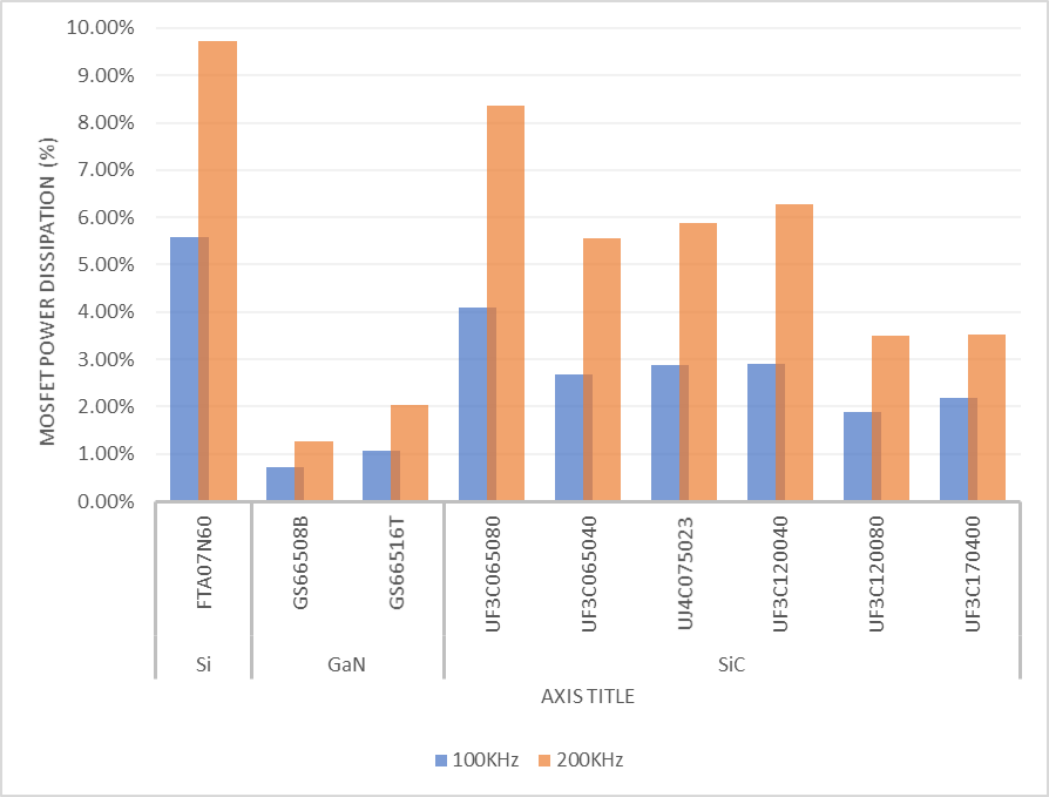

Figure 25. Effect of MOSFET power dissipation on efficiency, operating @100V

4.2 Flyback Converter Without RC Snubber and Clamp Circuit

As mentioned previously, RC snubber and clamp circuits protect the power semiconductor device but also affect the design's efficiency. The subsections below will demonstrate the findings of the simulation study implemented on Si, GaN, and SiC.

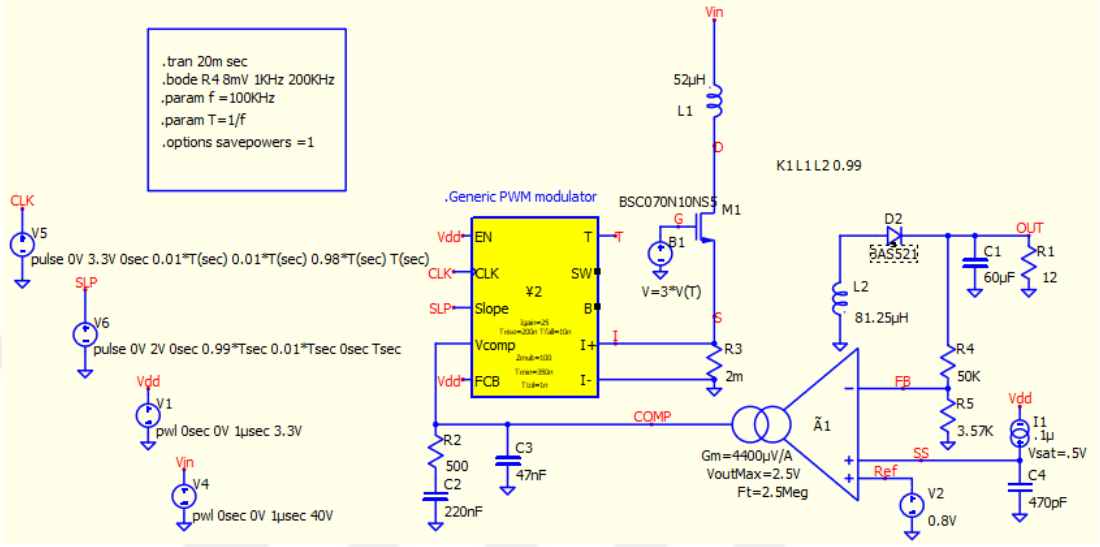

Figure 26. Flyback power converter design without RC and clamp circuits

Figure 26 above illustrates the complete design of a Flyback power converter with peak current mode control. However, the RC snubber and Clamp circuits are excluded from the design for testing and evaluating the performance of semiconductor electronic devices.

4.2.1 Silicon-type MOSFETs

Table 18

Simulation Results of Silicon (Si) Mosfets Operating at Vds= 40V and Fs= 100KHz & Fs= 200KHz

Switching freq.	Device Model	Vout (V)	Drain voltage (V)	Efficiency (%)	Power Diss. (W)	Temp. (C°)
100KHz	FTA07N60	12	App. 220 V	81%	0.673791	29.70
200KHz	FTA07N60	12	App. 180 V	81%	0.68345	29.73

Table 19

Simulation Results of Silicon (Si) Mosfets Operating at Vds=100V and Fs= 100KHz & Fs= 200KHz

Switching freq. (Hz)	Device Model	Vout (V)	Drain voltage (V)	Efficiency (%)	Power Diss. (W)	Temp. (C°)
100KHz	FTA07N60	12	App. 220 V	82%	0.419399	28.68
200KHz	FTA07N60	12	App. 220 V	79.8%	0.631111	29.52

4.2.2 Gallium nitride-type MOSFETs

Table 20

Simulation Results of GaN Mosfets Operating at Vds= 40V, Fs= 100KHz

Device Part no.	Output voltage(V)	Drain voltage(V)	Efficiency (%)	Power Diss. (W)	Temp. (°C)
GS66508B	12	App. 350 V	88.3%	0.0460738	27.02
GS66516T	12	App. 350 V	88.5%	0.0885549	27.02

Table 21

Simulation Results of GaN Mosfets Operating at Vds= 40V, Fs= 100KHz

Device Part no.	Output voltage(V)	Drain voltage(V)	Efficiency (%)	Power Diss. (W)	Temp. (°C)
GS66508B	12	App. 180 V	88.00%	0.0460738	27.02
GS66516T	12	App. 180 V	87.1%	0.226481	27.06

Table 22

Simulation Results of GaN Mosfets Operating at Vds= 100V, Fs=100KHz

Device Part no.	Output voltage(V)	Drain voltage(V)	Efficiency (%)	Power Diss. (W)	Temp. (°C)
GS66508B	12	App.550 V	88.18%	0.0453042	27.02
GS66516T	12	App. 420 V	87.8%	0.182588	27.05

Table 23

Simulation Results of GaN Mosfets Operating at Vds= 100V, Fs= 200KHz

Device Part no.	Output voltage(V)	Drain voltage(V)	Efficiency (%)	Power Diss. (W)	Temp. (°C)
GS66508B	12	App. 400 V	86.30%	0.0596378	27.03
GS66516T	12	App. 350 V	84.3%	0.616915	27.17

4.2.3 Silicon carbide-type MOSFETs. Tables 24, 25, 26, and 27 below outline the performance of SiC-based MOSFETs in a flyback power converter circuit design, excluding the RC snubber and clamp circuit.

Table 24

Simulation Results of SiC Mosfets Operating at Vds= 40V, Fs=100KHz

Device Part no.	Output voltage(V)	Drain voltage(V)	Efficiency (%)	Power Diss. (W)	Temp. (°C)
UF3C065040	12	App. 160 V	87.20%	0.104444	27.05
UF3C065080	12	App. 330 V	87.80%	0.113031	27.12
UJ4C075023	12	App. 215 V	87.0%	0.127493	27.06
UF3C120040	12	App. 210 V	86.2%	0.200478	27.07
UF3C120080	12	App. 280 V	88.0%	0.105449	27.04
UF3C170400	12	App. 660 V	86.70%	0.282883	27.42

Table 25

Simulation Results of SiC Mosfets Operating at Vds= 40V, Fs= 200KHz

Device Part no.	Output voltage(V)	Drain voltage(V)	Efficiency (%)	Power Diss. (W)	Temp. (°C)
UF3C065040	12	App. 190 V	85.40%	0.241276	27.11
UF3C065080	12	App. 250 V	86.60%	0.203595	27.22
UJ4C075023	12	App. 180 V	84.0%	0.553323	27.27
UF3C120040	12	App. 160 V	85.0%	0.336591	27.12
UF3C120080	12	App. 250 V	86.7%	0.170068	27.06
UF3C170400	12	App. 200 V	86.13%	0.291635	27.44

Table 26

Simulation Results of SiC Mosfets Operating at Vds= 100V, Fs= 100KHz

Device Part no.	Output voltage(V)	Drain voltage(V)	Efficiency (%)	Power Diss. (W)	Temp. (°C)
UF3C065040	12	App. 300 V	85.30%	0.242655	27.11
UF3C065080	12	App. 400 V	86.67%	0.153704	27.17
UJ4C075023	12	App. 280 V	85.0%	0.301214	27.15
UF3C120040	12	App. 280 V	85.0%	0.284424	27.10
UF3C120080	12	App. 345 V	86.6%	0.15026	27.05
UF3C170400	12	App. 660 V	87.00%	0.147816	27.22

Table 27

Simulation Results of SiC Mosfets Operating at Vds= 100V, Fs=200KHz

Device Part no.	Output voltage(V)	Drain voltage(V)	Efficiency (%)	Power Diss. (W)	Temp. (°C)
UF3C065040	12	App. 260 V	83.20%	0.24747	27.11
UF3C065080	12	App. 330 V	83.67%	0.226784	27.25
UJ4C075023	12	App. 245 V	80.2%	1.04388	27.51
UF3C120040	12	App. 280 V	82.1%	0.430568	27.15
UF3C120080	12	App. 300 V	83.6	0.224869	27.08
UF3C170400	12	App. 550 V	84.70%	0.194997	27.29

4.2.4 Si, GaN, &SiC overall comparison. Figures 27, 28, 29, and 30 below present graphs derived from the tables above, simplifying comparisons in the discussion chapter.

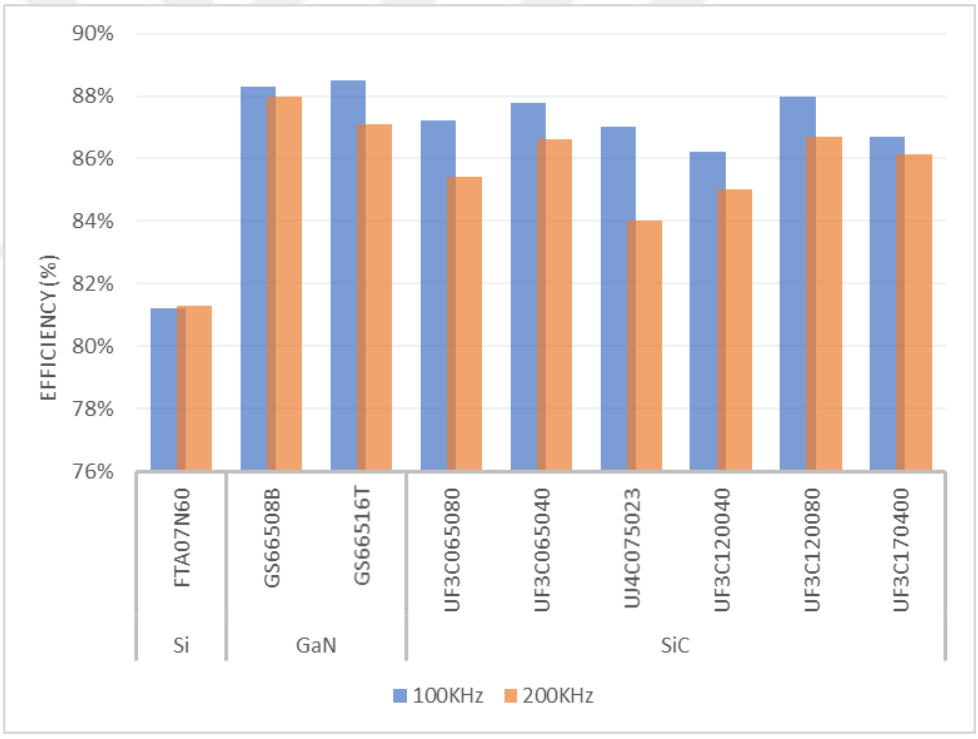

Figure 27. Efficiency plot of Si, GaN, & SiC devices operating at Vds= 40V

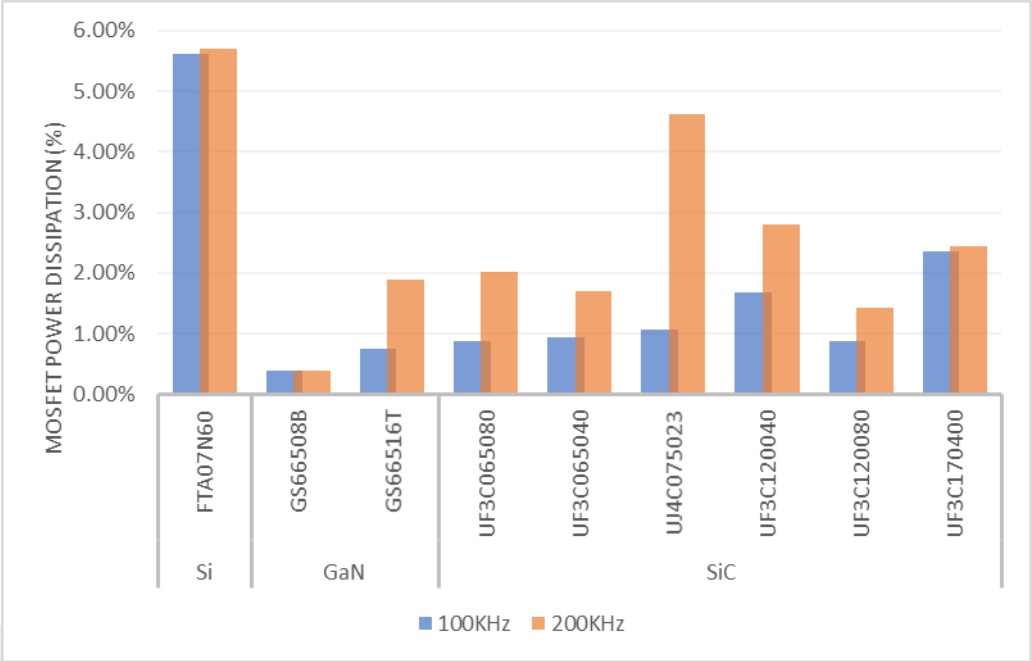

Figure 28. Effect of MOSFET power dissipation on efficiency, operating at 40V

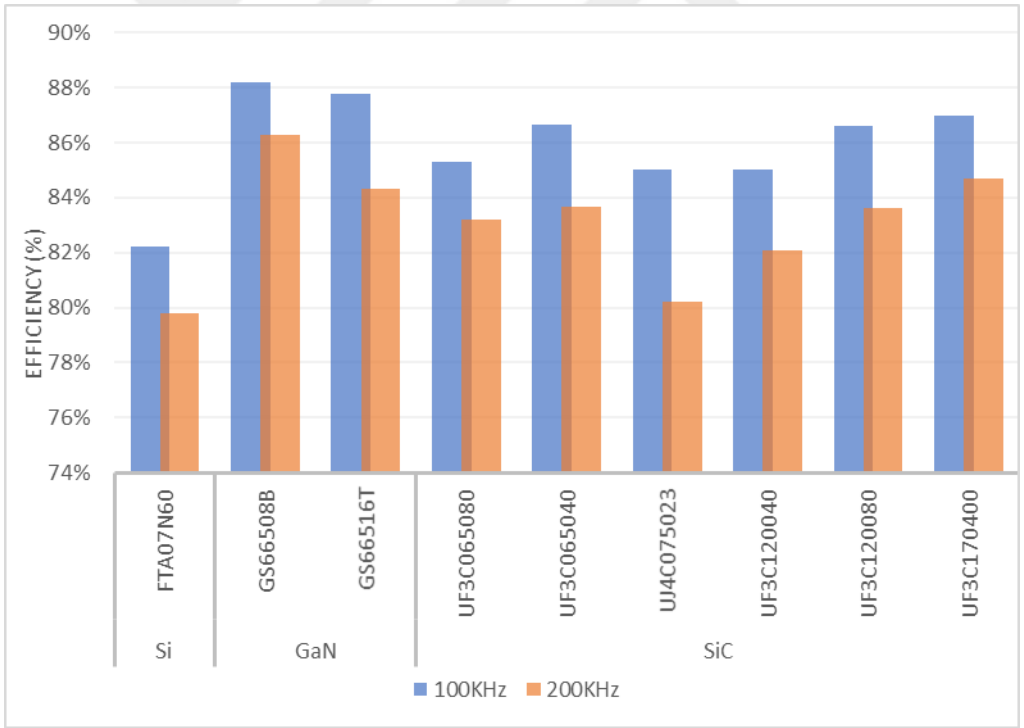

Figure 29. Efficiency plot of Si, GaN, & SiC devices operating at Vds= 100V

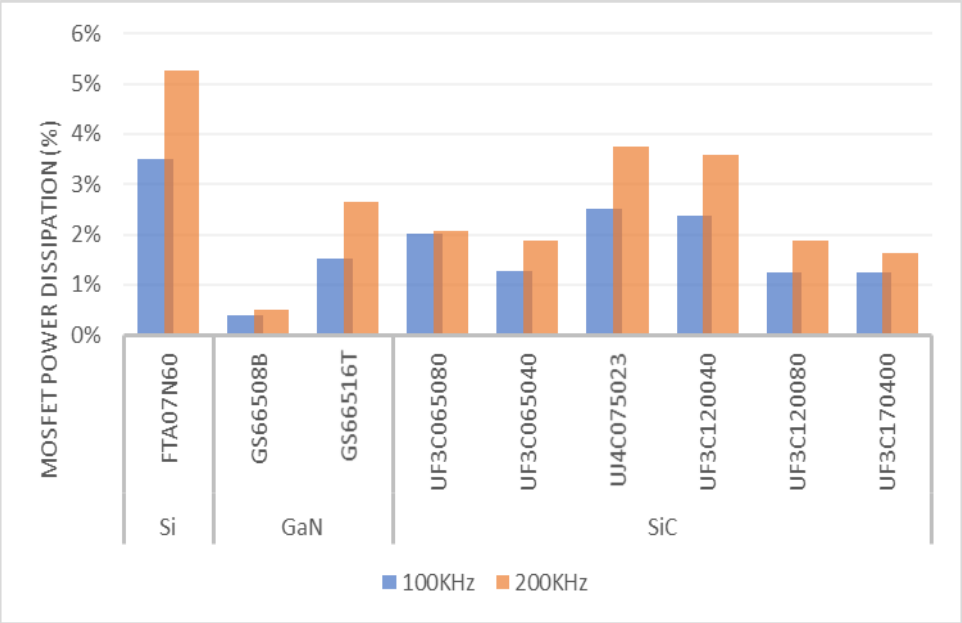

Figure 30. Effect of MOSFET power dissipation on efficiency, operating at 100V

4.3 Cost Analysis of Chosen MOSFETs

Table 28 below illustrates the market prices of the Si, GaN, and SiC MOSFETs chosen for the simulation comparison study.

Table 28

Market Prices for the Chosen Mosfets (Mouser Electronics, 2024)

S. N	Device part no.	Type	Market Price €
1	BSC070N10NS5	Si	0.88602
2	SQ3426EEV	Si	0.287
3	BSC123N08NS3	Si	0.566
4	FTA07N60	Si	3.36
5	EPC2218	GaN	3.17
6	GS66508B	GaN	17.42
7	GS66516T	GaN	33.1
8	UF3C065040	SiC	9.04
9	UF3C065080	SiC	5.53
10	UJ4C075023	SiC	10.16
11	UF3C120040	SiC	19.72
12	UF3C120080	SiC	8.85
13	UF3C170400	SiC	5.16

Chapter 5

Discussion and Conclusion

5.1 Discussion of Simulation Findings

The quality of a semiconductor device is determined by its performance in applications. The choice of a semiconductor material depends on which type best meets the application's specific requirements. Referring to the simulation findings obtained by QSPICE, devices have been tested under various operating conditions, and their findings will be discussed in this chapter.

5.1.1 Flyback converter with RC snubber and clamp circuit. Figures 22, 23, 24, and 25 summarize data from several comparison tables in subsection 4.1. Figure 22 shows the efficiency characteristics of silicon (Si), gallium nitride (GaN), and silicon carbide (SiC) MOSFETs at a drain-source voltage (Vds) of 40V and switching frequency of 100kHz and 200kHz. The Si devices operate at moderate efficiency, varying between 78% and 83% at an operating frequency of 100kHz. Silicon devices' efficiency decreases to the range between 76% to 79.7% at 200kHz due to switching losses, which are insensitive to high frequencies and prove the inefficiency of silicon usage in high-frequency applications. The GaN devices were observed to have high efficiency at 40V. The efficiency was recorded to vary between 82% to 83% when operating at 100KHz. At 200KHz, the efficiency was around 80% for all GaN devices. Furthermore, newly developed SiC devices are close in efficiency to both Si and GaN at 40V. The efficiency ranges between 80% to 83% at 100KHz and 78% to 80% at 200KHz.

Even though SiC and GaN both had a good range of efficiency at both switching frequencies, the efficiencies were expected to be higher. The reason is that at low frequencies, the conduction losses dominate the total losses in a system. For example, Referring to Table 6 in section 3.2, the silicon mosfet (BSC070N10NS5) has a drain to source on resistance of 6 mΩ, whereas GaN (EPC2218) and SiC (UJ4C075023) have a R_{ds-on} of 2.4mΩ and 23mΩ, respectively. Figure 23 demonstrates a closer study of the MOSFET power dissipation effect on the design's efficiency. If we compare the above-mentioned MOSFETs, it is noticed that Si mosfet has a power dissipation percentage of 0.72%, GaN recorded 0.39%, and SiC is affected by 0.93% when operating at 100 kHz. These values indicate that silicon devices are reasonably

efficient at lower frequencies. Still, the FTA07N60, a high-voltage silicon device, amounts to 6.29%, which indicates significant energy losses at moderate frequencies. This proves that specific silicon designs are imperfect in applications where efficiency is crucial. As the switching frequency increases to 200 kHz, the dissipation percentages for all MOSFETs increase due to the more significant switching losses. Even here, the FTA07N60 based on silicon has a marked effect because power dissipation reaches 6.95%. On the other hand, the dissipation effect of other devices, such as the BSC070N10NS5 and BSC123N08NS3, rises to about 1.42% and 1.09%, respectively. GaN MOSFET devices recorded the lowest power dissipation factor compared to Si and SiC. For instance, EPC2218, GS66508B, and GS66516T show dissipation rates of 0.39 % or 0.43 % at 100KHz. Nonetheless, at 200 kHz, their loss is slightly increased to 0.54% and 0.78%. These results demonstrate GaN's efficiency for designs with high switching frequencies. Furthermore, silicon carbide (SiC) MOSFETs – including the UF3C and UJ4C series – are positioned between silicon and GaN devices. The dissipated power percentage at 100 kHz ranges between 0.93% – 2.67 %, and at 200 kHz, in the range of 1.37 % – 2.92 %. SiC devices are used where voltage and temperature capabilities are critical because they have better higher power use characteristics. However, their dissipation rates are comparatively higher than those of GaN devices. This trade-off indicates that SiC devices are appropriate for applications where thermal stability and voltage performance are more important than efficiency.

Figure 24 depicts the performance of the same semiconductor materials at a higher 100V drain to source voltage but at the same switching frequency. The efficiency levels of the Si devices are much lower than their values at 40V. For example, the FTA07N60 MOSFETs are the only MOSFET of this type that can tolerate 100V V_{ds} out of all the mentioned types of Si-type MOSFETs, provided that some of them have maximum V_{ds} of 100V, and some are even lower. FTA07N60 achieves an efficiency rating of 77% at 100kHz and 71.5% at 200kHz. This reduction shows that the switching losses of silicon increase as the operating voltage increases, making the technology unsuitable for high-voltage applications.

However, GaN devices do not allow degradation of their superior performance up to 100V. Devices like the GS66508B and GS66516T effectively deliver their

services with an efficiency rate of 78.8% at 100KHz, and 79.2% at 200KHz. This proves GaN's efficiency in managing high-frequency and high-voltage operations.

SiC devices remain superior at 100V in terms of efficiency and operate with the best effectiveness of the three material types. Specific examples of devices are UJ4C075023 and UF3C120080, which operate with an efficiency of 79.2% and 79% at 100 kHz, and 73.4% and 74% at 200 kHz, respectively. High conduction and switching losses are not an issue for SiC, thus retaining the highest efficiency level when working at significant voltage levels, evoking it as the best decision for critical use. Lastly, Figure 25 demonstrates the effect of MOSFET power dissipation on the system efficiency when operating at 100V and switching frequencies of 100KHz and 200KHz. Si MOSFET, represented by FTA07N60, has the highest power dissipation with a considerable rise from 5.58% at 100 kHz to nearly 10% at 200 kHz. This steep increase proves the inability of silicon MOSFETS to operate efficiently under high voltages and high-frequency circuit designs. In contrast, GaN MOSFETs demonstrated significantly low power loss, with ratios of 0.71% and 1.07% at 100 kHz. The second evaluation test was performed with the switching frequency increased to 200 kHz, but the change was negligible as the power dissipation increased to 1.26% and 2.04% only.

Intermediate performers are SiC MOSFETs under models like UF3C065080, UF3C065040, and UF4C075023. For instance, the characteristic of the model UF3C065080 dissipation circuit increases from 4% at 100 kHz to 8.37% at 200 kHz. Meanwhile, other SiC devices, like the UF3C120080 MOSFET type, exhibit lower ratios of 1.88% at 100KHz and 3.5% at 200KHz.

To sum up, the benefit of having a higher frequency operation is that it helps achieve smaller designs with high efficiency by reducing the transformer size and output capacitor. Furthermore, each MOSFET has its own drain-to-source capacitance. Changing the MOSFET type will affect the drain's ringing frequency for any designed circuit. Upon this, the RC snubber should be redesigned depending on the type of MOSFET.

5.1.2 Flyback converter without RC snubber and clamp. Circuits Figures 27, 28, 29, and 30 summarize the data given in Tables 18 to 27. The graph in Figure 27 illustrates the efficiency of silicon (Si), gallium nitride (GaN), and silicon carbide (SiC) semiconductor devices operating at a drain-to-source (V_{ds}) voltage of 40V and

switching frequencies of 100KHz and 200KHz. From the displayed graph, the GaN devices yield the highest efficiency among all three types of material at both switching frequencies. For instance, GS66508B and GS66516T exhibit improved efficiency characteristics higher than 88% at a frequency of 100 kHz. Furthermore, GaN proved its suitability for high-frequency applications, achieving impressive efficiency values of 88% for the GS66508B and 87% for the GS66516T at 200KHz. This illustrates the benefits of GaN technology, including low switching losses and high electron mobility. Likewise, SiC devices performed well and achieved high-efficiency levels at both switching frequencies. For example, the UF3C120080 and the UF3C065040 are as high as 88% at 100KHz, and 87% at 200KHz. Most of the studied SiC devices maintained a robust performance at 200 kHz, although an efficiency of around 84 % was recorded for specific models such as the UJ4C075023 compared to other devices. However, this efficiency level can still be considered to be satisfactory. On the other hand, silicon devices (FTA07N60A) show the lowest efficiency among the three types of materials at both frequencies, around 81%. These results demonstrate the issues associated with silicon technology at higher frequencies and power levels, such as emerging switching losses. In addition, Figure 28 gives a better understanding of the MOSFET performance and its effect on the overall design efficiency. It can be seen that Si-based MOSFET recorded the worst percentage of around 5.6% to 5.7% in both operating frequencies. GaN had the lowest range, with less than 1% at 100KHz and less than 2% at 200KHz. SiC performed well in lower frequencies compared to higher frequencies. However, the percentage of effect is acceptable.

Figure 29 depicts the performance of the same semiconductor materials at 100V drain to source voltage while maintaining the same switching frequency, 100KHz and 200KHz. These efficiency trends show a difference when compared to the previous graph at 40V. GaN devices continue outperforming SiC and Si devices, securing their position as the optimal choice for high-frequency applications. At 100 kHz, the efficiency is about 88% for both devices. Moreover, at 200KHz, the efficiency is 86% for GS66508B and 84% for GS66516T. Compared to 40V, it is noted that the GaN device's efficiency decreased only by a factor of 2% at 200KHz while maintaining nearly the same high efficiency at 100KHz. These results show that GaN can offer a better improvement in switching losses at the higher voltage side of the system's

overall efficiency. SiC devices also demonstrate a High efficiency, but their efficiency appears to be slightly worse at 200 kHz than at 100 kHz. For example, the UF3C120080 and UF3C170400 are nearly 87% at 100 kHz, while at 200 kHz, they showed around 84% and 85% efficiency rates, respectively. On the other hand, the UJ4C075023 exhibits a greater fall in efficiency and reaches approximately 80% at 200KHz compared to the initial efficiency of 85%. These results confirm the high sensitivity of SiC devices to switching losses at higher frequencies. However, their behavior is still acceptable, especially in high-power applications. Generic silicon devices have been observed as being far much slower than GaN and SiC electronic devices when operated under both switching frequencies. The FTA07N60 has 82% efficiency at 100 kHz, which decreases to approximately 79.8% at 200 kHz. Also, in Figure 30, the effect of using Si-based MOSFETs in high power and frequency is noticed. GaN and SiC showed extremely lower percentages of power dissipation compared to Si-based.

Consequently, the conduction losses are proportional to the material's Rds-on range. Specifically, SiC devices are characterized by having higher Rds-on ranges than GaN. Thus, their conduction losses are more elevated when operating at low switching frequencies. Also, the switching losses become the dominant total losses at the higher switching frequency. GaN has a lower gate charge and parasitic capacitances, which reduces the energy loss during switching. Moreover, GaN's high electron mobility enables faster switching transition than Si and SiC. On the other hand, SiC devices possess high thermal resistance and power levels, making them a favorite for high voltage and power applications. Concerning silicon, some silicon devices have a very high R_{ds-on} range, meaning that they are not very suitable for use in high-power and voltage applications. Nevertheless, the advantage of SiC over Si decreases as frequency and power get lower. Therefore, based on the above comparison, silicon seems to be more viable in low-frequency and power electronics applications.

Table 28 lists the market prices of the chosen MOSFETs to study and analyze the economic factors. When it comes to cost, the highest price was identified in GaN-based MOSFETs, while Si-based MOSFETs were the most cost-effective. SiC falls in between GaN and Si. Nonetheless, the difference in prices between the devices is not

very significant, meaning that a better design with higher efficiency, improved overall performance, and longer life designs is more important than cost.

5.2 Conclusion

This thesis focuses on comparing the performance of Si, SiC, and GaN MOSFETs in a Flyback converter with 100kHz and 200kHz switching frequencies and 40V and 100V operating voltages. GaN has the highest efficiency at higher frequencies and medium to high voltage applications. This is because of its high electron mobility and its ability to offer low switching loss characteristics. SiC works well at moderate frequency applications but has proved its excellence and is better suited for devices working at high power applications. Conversely, Silicon is useful in low frequencies and voltages, though it has low efficiency in higher frequencies and high voltages. This showcases GaN and SiC materials as industry favorites for high-frequency and high-power uses, while silicon is preferred for low-frequency and low-voltage applications.

5.3 Future Work

As future work, diamond may be investigated as a new semiconductor material for power electronics, given its low thermal resistance, high breakdown voltage, and excellent electron mobility to outperform SiC and GaN for high-power applications. Furthermore, it is possible to automate the simulation procedure for the evaluation of hundreds or thousands of different models of MOSFET and extend the analysis, enlarge the results base, and give a more profound evaluation of various kinds of semiconductor materials under the given conditions with the aim to further improve the performance of power electronic systems.

REFERENCES

Ahmed, O., Khan, Y., Butt, M. A., Kazanskiy, N. L., & Khonina, S. N. (2022). Performance Comparison of Silicon- and Gallium-Nitride-Based MOSFETs for a Power-Efficient, DC-to-DC Flyback Converter. *Electronics*, *11*(8). MPDI. https://doi.org/10.3390/electronics11081222

Analog Devices. (2024). LTC3805-5 datasheet. Retrieved from Datasheet4u.com website: https://www.datasheet4u.com/share_search.php?sWord=LTC3805-5

C, N., Sreedevi, A., & Gopal, M. (2015). Simulation and hardware implementation of 24 watt multiple output Flyback converter. *2015 International Conference on Power and Advanced Control Engineering (ICPACE)*. Bengaluru, India: IEEE.

Czarkowski, D. (2011). *Power Electronics Handbook (Third Edition)* (Third, pp. 249–263). Science Direct.

Glashauser, michael, & Kreutzer, Ing. (2023). Why Are Conventional Si MOSFETs Better Than SiC and GaN in Low Power Applications? *IEEE*. Presented at the 2023 IEEE Workshop on Wide Bandgap Power Devices and Applications in Asia (WiPDA Asia), Hsinchu, Taiwan.

Halder, T. (2017). A Comparative Study of Control Strategies for the Flyback SMPS . *2016 7th India International Conference on Power Electronics (IICPE)*. India: IEEE.

Hoddeson, L. (1981). The Discovery of the Point-Contact Transistor. *Historical Studies in the Physical Sciences*, *12*(1), 41–76. https://doi.org/10.2307/27757489

Kanthimathi, R., & Kamala, J. (2015). Analysis of different Flyback Converter Topologies. *2015 International Conference on Industrial Instrumentation and Control (ICIC)*, 1248–1252. India: IEEE.

Kewei, H. ’, Jie, L., Ningjun , F., Yuebirr, L., Xiaolirr, H., & LuO, W. (2009). Modeling Analysis and Simulation of High-voltage Flyback DC-DC Converter. *2009 IEEE International Symposium on Industrial Electronics*, 813–818. korea: IEEE.

Mouser electronics. (2024). MOSFETs – Mouser Europe. from Mouser.com website: https://eu.mouser.com/c/semiconductors/discrete-semiconductors/transistors/mosfets/

Nambiar, V., Yahya, A., & Selvaduray, T. (2012). *SPICE modelling of a valley switching flyback power supply controller for improved efficiency in low cost devices*. 10–14. https://doi.org/10.1109/iccircuitsandsystems.2012.6408340

Picard, J. (2010). *Under the Hood of Flyback SMPS Designs* (p. 261). Google scholar : TEXAS INSTRUMENTS . Retrieved from TEXAS INSTRUMENTS website:https://www.mikrocontroller.net/attachment/202520/Under_the_Hood_of_Flyback_SMPS_Designes_slup261__TI.pdf

Pullabhatla, S., Bobba, P., & Yadlapalli, S. (2020). Comparison of GAN, SIC, SI Technology for High Frequency and High Efficiency Inverters. *E3S Web of Conferences*, *184*. EDP Sciences.

Rai, S. (2020). GaN, SiC or Silicon Mosfet – A Comparison Based On Power Loss Calculations. *PCIM Asia* . Presented at the PCIM Asia 2020; International Exhibition and Conference for Power Electronics, Intelligent Motion, Renewable Energy and Energy Management, Shanghai, China.

RAJU, D. (2020). *Design of Gallium Nitride MOSFET based DC/DC converter* (Thesis). CHALMERS UNIVERSITY OF TECHNOLOGY.

SBURLAN, I., VASILE, I., & TUDOR, E. (2021). Comparative study between semiconductor power devices based on silicon Si, silicon carbide SiC and gallium nitrate GaN used in the electrical system subassembly of an electric vehicle . *IEEE*. Presented at the 2021 International Semiconductor Conference (CAS), Romania.

Shah, F., Xiao, H., Li, R., Awais, M., Zhou, G., & Bitew, G. (2018). Comparative Performance Evaluation of Temperature Dependent Characteristics and Power Converter using GaN, SiC and Si Power Devices . *IEEE*. Presented at the 2018 IEEE 12th International Conference on Compatibility, Power Electronics and Power Engineering (CPE-POWERENG 2018), QATAR, DOHA.

Sheng, K., & Guo, Q. (2012). Recent Advances in Wide Bandgap Power Switching Devices. *ECS Transactions*, *50*(3), 179–188. The Electrochemical Society. https://doi.org/10.1149/05003.0179ecst

Shetty, N., & Kumar, P. (2017). Simulation of Flyback Converter with Peak Current Mode Control. *IJIREEICE*, *5*(2), 78–83.

Yang, V. (2016, May). Peak Current Mode and Continuous Current Mode DC-to-DC Converter Modeling and Loop Compensation Design Considerations. Retrieved from Analog.com website: https://www.analog.com/en/resources/technical-articles/peak-current-mode-and-continuous-current-mode-dc-dc-converters.html